USING ISOPYCNIC EQUILIBRIUM SEDIMENTATION TO EXPLORE *CRYPTOCOCCUS NEOFORMANS* BIOLOGY

BY

RAGHAV VIJ

A thesis submitted to Johns Hopkins University in conformity with the requirements for the degree of Master of Science

Baltimore, Maryland

April 2018

ABSTRACT

Cryptococcus neoformans is an environmental fungal pathogen that disseminates to the brains of immunocompromised individuals causing a fatal meningeal disease. Of the major virulence factors studied, the polysaccharide capsule that extends radially from the cell wall, and the pigment melanin deposited between the cell-wall and cell-membrane of *C. neoformans* are amongst the most important.

Historically, isopycnic equilibrium sedimentation has been used for the separation of different kinds of cells and for the isolation of subcellular components. We believe that the buoyant cell density of a microbial cell is an important physical characteristic that may affect its transportability in fluids and interactions with tissues during infection We report on the variance of buoyant cell density in strains belonging to *C. neoformans* and *C. gattii* species complexes. Our results suggest that the polysaccharide capsule contributes to lowering the yeast's cell density. The low buoyant density of *C. neoformans* due to capsule induction conceivably allows the fungi to float in aquatic reservoirs and could facilitate environmental dispersal. Furthermore, the binding of certain capsular antibodies and melanization also mildly affect the buoyant density of the cells could contribute to altering the dissemination of the fungal pathogen.

Melanin is another important virulence factor in many pathogenic fungi, including *C. neoformans*. Furthermore, extracellular vesicles are often seen as virulence bags that carry proteins and enzymes that are important for *C. neoformans* pathogenesis. In this study we report the discovery of secreted "melanin granules" that are similar in size to extracellular vesicles (50-80 nm) and yet can be separated from vesicles by density gradient (isopycnic) ultracentrifugation. Cell-wall associated melanin isolated from *C. neoformans*, called “melanin ghosts”, is comprised of granular structures stacked in concentric layers. Chemical and mechanical disruption of “melanin ghosts” results in melanin nanoparticles that are also granular and have a similar size distribution to that of melanin granules isolated from the supernatant of melanized cultures. This has lead us to hypothesize that the secreted melanin granules are the fundamental unit of fungal melanin found on the cell-wall of the yeast. Studying the proteins and lipids associated with the secreted melanin granules could provide us insights into fungal melanogenesis and lead to novel therapeutic targets to control *C. neoformans* infection.

ACKNOWLEDGMENT

I am grateful for having been given an opportunity to earn my Master of Science (ScM) at the Department of Molecular Microbiology and Immunology, Johns Hopkins Bloomberg School of Public Health. I had first come across Dr. Arturo Casadevall's work on microbial pathogens during my undergraduate studies at Amity Institute of Biotechnology, Amity University NOIDA, India. I was very excited when he allowed me to join his laboratory to allow me to complete the research and thesis requirements for my ScM program under his aegis. Under his stewardship, I learned to formulate my own research project and exercise creative freedom in research. He truly instilled his philosophy of scientific research in me.

I was also mentored by a senior member of Dr. Casadevall's laboratory, Dr. Radames J.B. Cordero. Words cannot convey my deep gratitude for his patience in teaching me essential laboratory, thinking and writing skills.

Importantly, I would like to thank Dr. Marie Hardwick for reading my thesis and providing insightful comments. I was fortunate enough to interact with her lab members when our labs shared a common space and developed a deep interest in her research and an appreciation for her rigorous methods in science. I have learned how to critically evaluate my own research, and the research of others by participating in the enriching discussions that take place during her lab journal club.

I would also like to extend my gratitude towards all faculty and staff, in particular to Ms. O'Connor who has patiently made sure that all of us cross over administrative hurdles with ease.

Further, my heartfelt love and gratitude to my parents, Lalit and Vidhu Vij, and my baby sister Ambika Vij, for their belief in me and continuing guidance and support.

I would also like to thank all other members of the laboratory. Dr. Carolina Coelho, Dr. Emma Camacho, Dr. Sarah Fu, Dr. Eric Jung, Diego D'Souza, Nina Grossman, Quigly Dragotakes, Ricardo Perez Gonzales, Kip Strother, and Dr. Maggie Wear for their support and friendship. They bored my oddities and each of them had invaluable lessons to impart to me.

I would like to thank my ScM cohort where I have found an excellent study group and some lifelong friends in Gaurav Dhiman, Andrew Yang and Emily Thompson. Many-a-thanks to Pravesh Parekh, Labani Biswas, Meghna Mathur and Rayhan Ghalib for their enriching and enduring friendship that has stood the test of time and distance.

Dr. Arturo Casadevall was supported by grants 5R01HL059842, 5R01AI033774, 5R37AI033142, and 5R01AI052733. We would like to thank Dr. Francoise Dromer (Institut Pasteur) for providing capsular antibody E1 (IgG).

TABLE OF CONTENTS

LIST OF FIGURES AND TABLES

Chapter 1: Isolation and characterization of melanin granules from *C. neoformans*

ABSTRACT

In the presence of catecholamine compounds, including L-DOPA found in the human brain, the fungi form a dark pigment called melanin that is deposited between the cell membrane and cell wall. This melanin coat is an important fungal virulence factor that is implicated in fungal defense mechanisms including resistance to host defense ROS, protection against antibody mediated phagocytosis and antifungal drugs. Although the contribution of *C. neoformans* melanin to virulence has been well studied, the structure and biogenesis of cryptococcal melanin remains elusive. Melanogenesis is believed to occur in intracellular spherical vesicular bodies called melanosomes and in fungi, the melanin coat is formed by a network of spherical nanoparticles organized into concentric layers that are stacked on top of another. In this study, we isolated and characterized melanin granules (50-80 nm) that were secreted by *C. neoformans* during melanization. We hypothesize that these nanoparticles are the fundamental units forming the melanin coat. We compared the biophysical characteristics of these secreted melanin granules and the cell wall-associated melanin. Melanin granules have the broadband optical absorption curve that is typical of melanin and aggregate in the presence of monovalent and divalent cations in a concentration dependent manner. Extensive sonication or acid hydrolysis of cell wall-associated melanin yield particles of similar size to the secreted melanin granules. Our data are consistent with the notion that secreted melanin granules

represent the fundamental structural unit of the *C. neoformans* melanin coat, which are released to the supernatant during the process of melanization. Future studies on these secreted melanin granules (i.e. lipid and protein composition) will provide valuable insights into the biogenesis and structure of fungal melanin, as well as, the potential role of melanin granules during infection.

INTRODUCTION

Melanins are dark polymeric pigments found in many species across the microbial and animal worlds serving multiple biological functions. This biopolymer is acid-resistant, exhibits a monotonic broadband optical absorption curve, is enriched in free radicals and exhibits ionic/electronic conductive properties (1). Thus, melanin finds wide-ranging applications in bioremediation, radioprotection, and formation of batteries and semiconductors (1, 2). To exploit the unique properties and find applications of microbial melanin, it is important to understand the biophysical characteristics of melanin and the process of its biogenesis.

Melanin is also an important virulence factor in many fungal pathogens, including *Aspergillus fumigatus*, *Cryptococcus neoformans*, *E. dermatiditis*, and *S. prolificans*. The pigment protects fungal pathogens against both abiotic stressors, such as physical (ionizing radiation), chemical (toxic metals, ROS), and mechanical (osmotic shock) assaults, and biotic environmental stressors (1).

The environmental yeast *C. neoformans* is most commonly found in pigeon guano and trees and has a wide range of natural hosts spanning the amoeba, birds and humans. *C. neoformans* is an important human pathogen that can cause pulmonary infections. In immunocompromised hosts, *C. neoformans* can disseminate from the lungs to the brain where it causes fatal meningeal disease leading to 181,100 deaths a year (3).

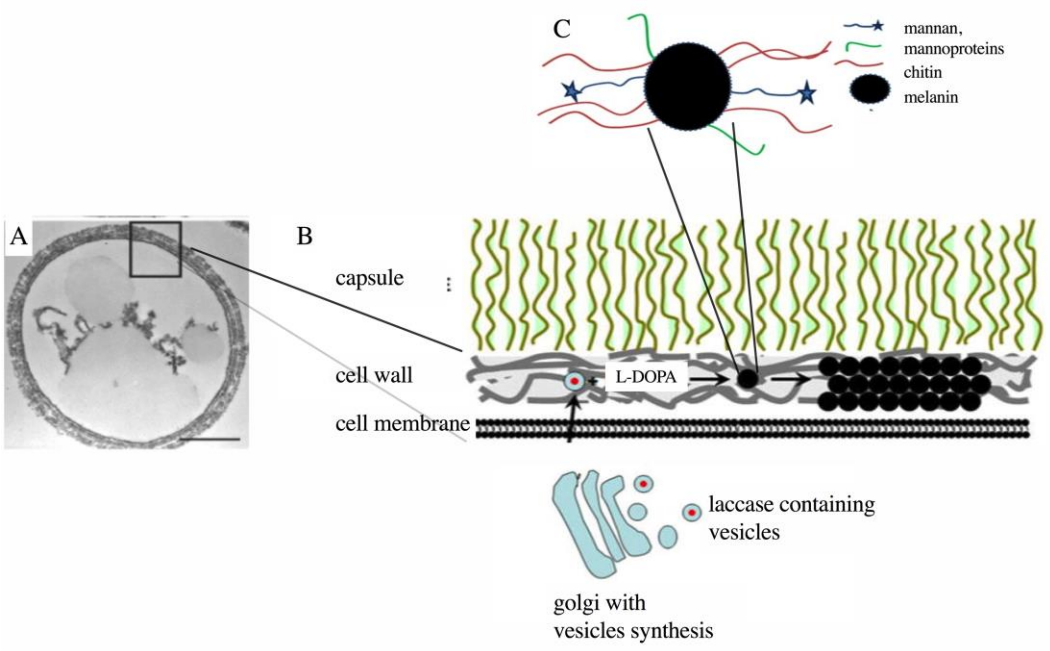

Figure 1.1: Melanin deposited on the *C. neoformans* cell wall. A. TEM section of a melanized *C. neoformans* "melanin ghosts" showing the deposition of melanin in concentric circles between the cell wall and cell membrane (Image taken from (4)). **B.** Proposed mechanism for deposition of melanin on the cell wall of *C. neoformans*. Vesicles emerging from the golgi (blue) and containing the enzyme laccase (blue with red) get transported through the cell membrane

(black bilipid layer) to the cell wall (grey lines). In the presence of melanin precursors (L-DOPA) these vesicles get melanized to form melanin granules and get anchored on to the cell wall. The capsule polysaccharide (green structure) emerge from the cell wall. **C.** On the cell wall granular structures are observed which may be secreted as melanin granules that may be associated to lipids, proteins, mannans and chitins that help anchor them to cell wall (modified model of fungal melanogenesis in *C. neoformans* taken from (5))

Melanin is an essential virulence factor and isolated melanin is sufficient to activate complement and induce inflammatory response in murine models (6). In *C. neoformans*, the polyphenol oxidase laccase catalyzes the one-step oxidation of precursor molecules (such as L-DOPA) that polymerize to form local ordered structures characterized by stacked indole groups like graphite. This is followed by the polymerization of the reactive intermediates that form disordered macromolecular arrangements that can culminate into spherical nanoparticles. In *C. neoformans*, melanin is deposited as concentric layers (**Figure 1.1A**) between the cell wall and the cell membrane. Since melanin is chemically strong, the cell-wall associated melanin can be isolated by removing the protein, lipid and nucleic acid components of the cell, followed by acid-hydrolysis, resulting in structures called melanin "ghosts" (**Figure 1.1A**) (7). Solid-state NMR studies of melanin ghosts from *C. neoformans* have revealed the association of many lipids, proteins and carbohydrates with melanin (8). An X-ray diffraction study showed that melanin associated with the cell wall of *C. neoformans* is composed of stacked

planar structures (like graphite) stabilized by π-π interactions (9). EM (Electron Microscopy) studies have revealed the microstructure of cell wall-associated melanin where spherical nanostructures ranging from 40-100 nm were observed on the surface of "melanin ghosts" (4). This observation had led to the hypothesis that melanogenesis occurs in vesicular structures (5), which was substantiated by the discovery that extracellular vesicles from *C. neoformans* can be melanized (10). Additionally, vesicles containing laccase, often localize near the cell wall of *C. neoformans* during infection, close to the site of melanin deposition (11). Furthermore, it is hypothesized that the oxidation of L-DOPA takes place inside vesicles to prevent intracellular toxicity due to free radical generation.

Recently, as part of an ongoing study, we have discovered melanin nanoparticles secreted by *C. neoformans* in medium containing L-DOPA. Biophysical characterization show that these melanin nanoparticles exhibit hydrodynamic sizes ranging from 40 to 70 nm in diameter and aggregate at high iconic strengths and hydrogen potential. We propose that these granular structures are the unit of the fungal melanin coat that is deposited on the cell wall. We show that prolonged acid hydrolysis and sonication of *C. neoformans* melanin ghosts produces particles that are similar in size, suggesting that the secreted melanin granules are the unit of *C. neoformans* melanin. Interestingly, *C. neoformans* mutants that lack enzymes involved in the formation of cell wall components, including chitosan synthase knockout mutants (12, 13) have a unique "leaky"

phenotype and are hypothesized to secrete melanin granules or laccase. Further investigation into the melanin granules from "leaky" mutants will allow us to characterize the cell biology of melanin formation in *C. neoformans.* This may lead to drugs that target melanin formation and control infection.

RESULTS

Isolation of secreted vesicles and melanin granules

A protocol for isolating extracellular vesicles was used to obtain vesicles, melanin granules from *C. neoformans* H99 strain grown in minimal medium with and without L-DOPA (**Figure 1.2A, C**), Laccase 1,2 knockout mutant with H99 background (Lac1,2 Δ) in minimal medium (**Figure 1.2B**) with L-DOPA. We observed vesicles ranging from 100-300 nm in H99 (+/- L-DOPA) and Lac1,2Δ using dynamic light scattering (DLS) (**Figure 1.2A-C, i**). Transmission electron microscopy (TEM) with negative staining showed the presence of electron dense aggregated granular structures that we call 'melanin granules' (**Figure 1.2A, ii**). Since L-DOPA auto-polymerizes, we also collected the L-DOPA aggregates from MM with L-DOPA and observed the presence of 70-100 nm (**Figure 1.2D, i**) aggregates of L-DOPA via DLS, however, under TEM we observed the presence of irregular and non-spherical aggregates that did not resemble melanin granules (**Figure 1.2D, ii**). Melanin has the unique ability to absorb almost every

wavelength of light, which results in a monotonic broadband absorption curve, and this curve is observed for the vesicles and melanin granule collected from H99 grown in MM with L-DOPA, but not for H99 grown in MM lacking L-DOPA (**Figure 1.3**). DLS also allows us to compute the dispersity index, a measure of the dispersion (or spread) of the estimated molar mass of colloidal particles in a solution (15, 16). We observed that the melanin granules had uniform dispersity as indicated by the low value, while the L-DOPA aggregates had non-uniform dispersity (**Table 1.1)**. This indicates that the two colloidal solutions have distinct characteristics, suggesting that the melanin granules isolated from *C. neoformans* are biologically synthesized.

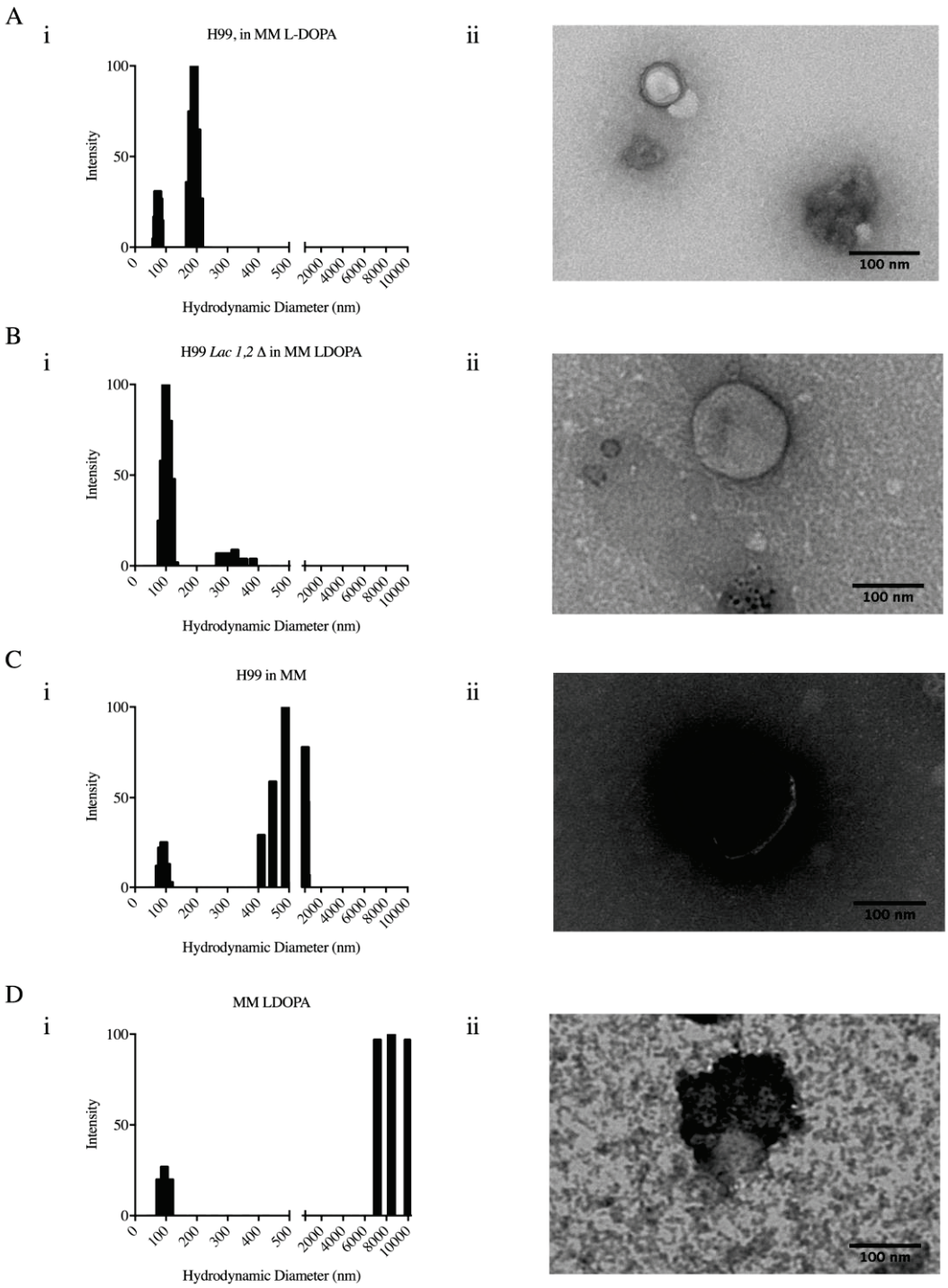

Figure 1.2: Secreted melanin granules and extracellular vesicles.

hydrodynamic diameter of vesicles and granules. **A.** *i*. Hydrodynamic diameter (by DLS) of vesicles and granules isolated from H99 grown in MM with L-DOPA. *ii*. Representative EM images from two independent experiments showing melanin granules (often present as aggregates) and vesicles. **B.** *i*. Hydrodynamic diameter and *ii*. EM images from vesicles isolated from laccase, 1,2 knock out grown in MM with L-DOPA from a single experiment. **C.** Hydrodynamic diameter and representative EM image of vesicles isolated from H99 grown in MM. **D.** *i.* Hydrodynamic diameter and *ii.* EM images of autopolymerized L-DOPA in MM from a single experiment. The scale bar represents 100 nm.

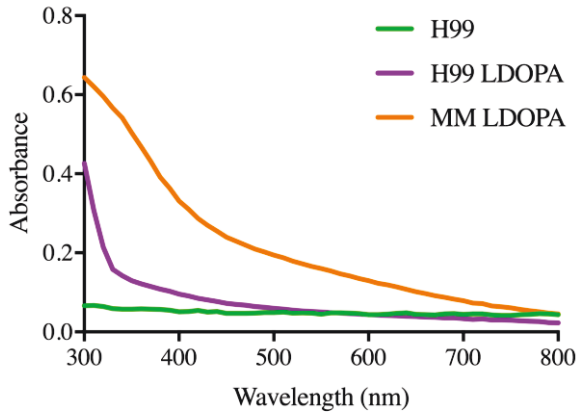

Figure 1.3: Absorbance spectra of vesicles and melanin granules. Melanin granules and vesicles collected from H99 grown in MM with L-DOPA (orange) has a broadband optical absorption curve which is characteristic of melanin. A curve for autopolymerized L-DOPA is apparent in MM (pink), and no such curve is visible for vesicles collected from H99 in MM lacking L-DOPA. Data is representative of two independent experiments.

Sample	Dispersity Index
H99	0.324
H99 + L-DOPA	0.094
H99 *Lac1, 2Δ*	0.093
L-DOPA	0.676

Table 1.1: Polydispersity of vesicles and granules. Melanin granules in H99 + L-DOPA had very low dispersity, suggesting that the population of melanin granules is highly monodispersed. L-DOPA aggregates had the highest dispersity.

Colloidal properties of melanin granules

We wished to characterize the colloidal properties of melanin granules, so that we may optimize buffers that prevent aggregation. In addition, the behavior of melanin granules in mono (Na^+) and divalent (Ca^{2+}) salt solutions may provide insights into the intramolecular interactions of melanin granules. We observed that crude pellet of H99 with L-DOPA, that contains melanin granules and vesicles, aggregated at >0.01M $CaCl_2$, >0.1M NaCl, >10X PBS (**Figure 1.4A-C**). The result suggests that divalent cations cause the aggregation or fusion event at lower concentrations than monovalent cations. This is consistent with studies on the phospholipid vesicles and liposomes that have suggested that divalent cations lead to vesicle fusion, and thus increase the size of particles in a solution (17, 18).

A

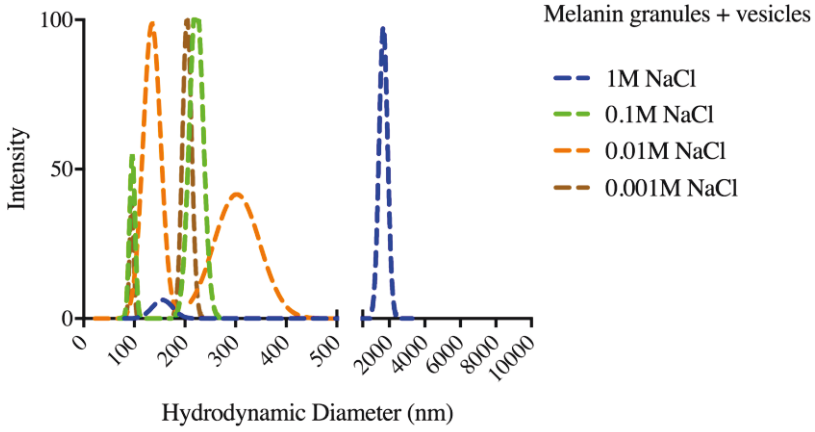
Melanin granules + vesicles
1M NaCl
0.1M NaCl
0.01M NaCl
0.001M NaCl
Intensity
100
50
0
0
100
200
300
400
500
2000
4000
6000
8000
10000
Hydrodynamic Diameter (nm)

B

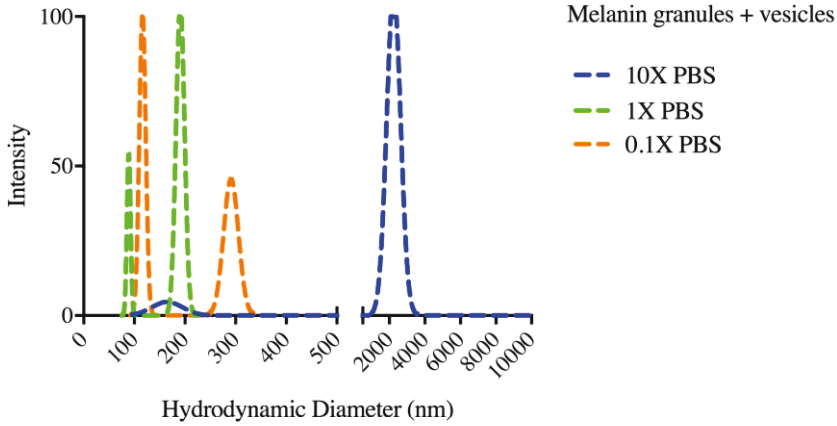
Melanin granules + vesicles
10X PBS
1X PBS
0.1X PBS
Intensity
100
50
0
0
100
200
300
400
500
2000
4000
6000
8000
10000
Hydrodynamic Diameter (nm)

C

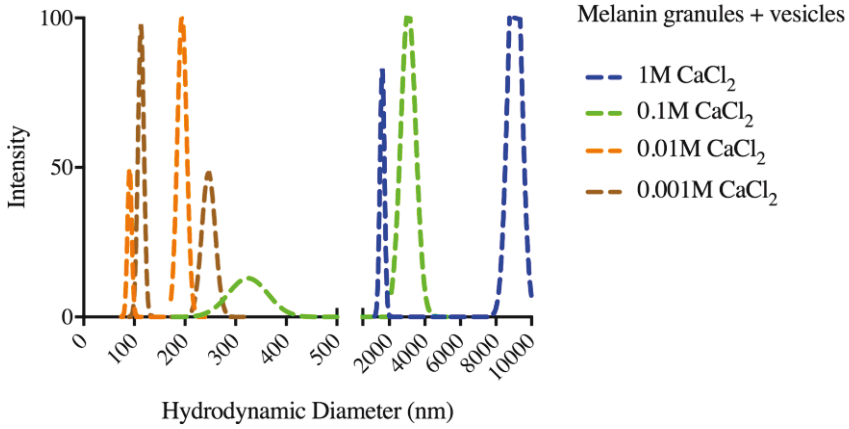
Melanin granules + vesicles
1M CaCl2
0.1M CaCl2
0.01M CaCl2
0.001M CaCl2
Intensity
100
50
0
0
100
200
300
400
500
2000
4000
6000
8000
10000
Hydrodynamic Diameter (nm)

Figure 1.4: Concentration dependent aggregation of melanin granules in the presence of divalent and monovalent cations. Representative data from two independent experiments depicting size distribution of melanin granules and vesicles collected from H99 grown in MM and LDOPA in **A.** 1M, 0.1M, 0.01M and **B.** 0.01M NaCl, $CaCl_2$, and in **C.** 10X, 1X and 0.1X PBS.

Isolation of melanin granules by density gradient ultracentrifugation

The pellet from ultracentrifugation of the supernatant from different sample cultures contains a mixture of vesicles, protein aggregates and, in the case of H99 + L-DOPA, melanin granules. We hypothesized that melanin granules would be tightly packed structures with high molecular weight and low volume and could be separated from vesicles and protein aggregates by buoyant density. Thus, we performed density gradient ultracentrifugation and collected the fractions. We observed vesicles from H99 +/- L-DOPA primarily in fractions 1 and 2 under TEM (**Figure 1.5B**). Upon ultracentrifugation of H99 +L-DOPA pellet, melanin granules were clearly visible as a dark band in fraction 5, and as aggregated electron dense structures under TEM (**Figure 1.5B**).

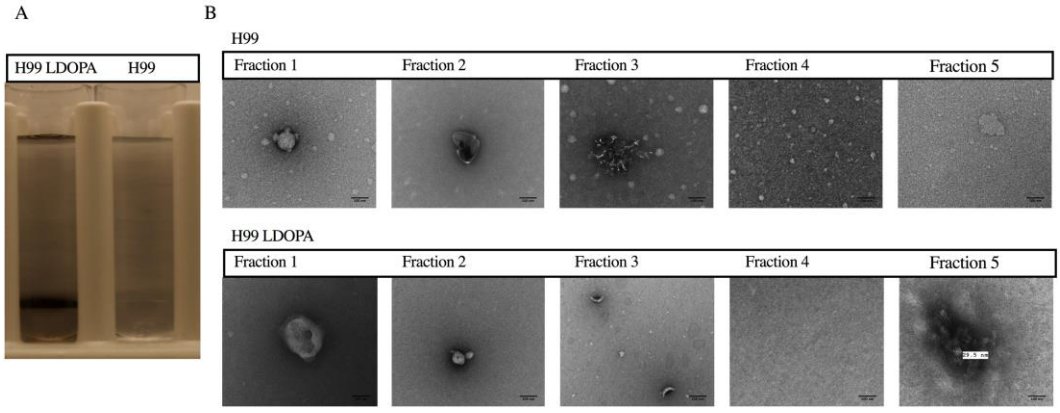

Figure 1.4: Density gradient separation of melanin granules from extracellular vesicles. A. Representative data from two independent experiments depicting an image of Optiprep density gradient ultracentrifugation of vesicles collected from H99 and vesicles + granules collected from H99 grown in MM with L-DOPA. **B.** Representative EM images from two independent experiments depicting Fractions 1-5 collected from density gradient centrifugation. Melanin granules are visible in fraction 5 of H99 + L-DOPA. The scale bar represents 100 nm.

Chemical and mechanical breaking down melanin "ghosts"

We hypothesized that the melanin granules found in the supernatant of H99 + L-DOPA are the unit of melanin found on the cell wall of melanized *C. neoformans*. Thus, we sought to break down the melanin ghosts isolated from the *C. neoformans* (7) by extended ultrasonication and prolonged-acid hydrolysis. We found that prolonged hydrolysis (2 weeks) of melanin ghosts resulted in particles of about 100-200 nm in size by DLS, while ultrasonication of melanin ghosts

resulted in particles of 0-200 nm (**Figure 1.6A, iv-vi**). An earlier study in Casadevall lab (by Rafael Prados-Rosales) had shown that prolonged hydrolysis resulted in particles that looked remarkably similar to the melanin granules we have isolated under TEM.

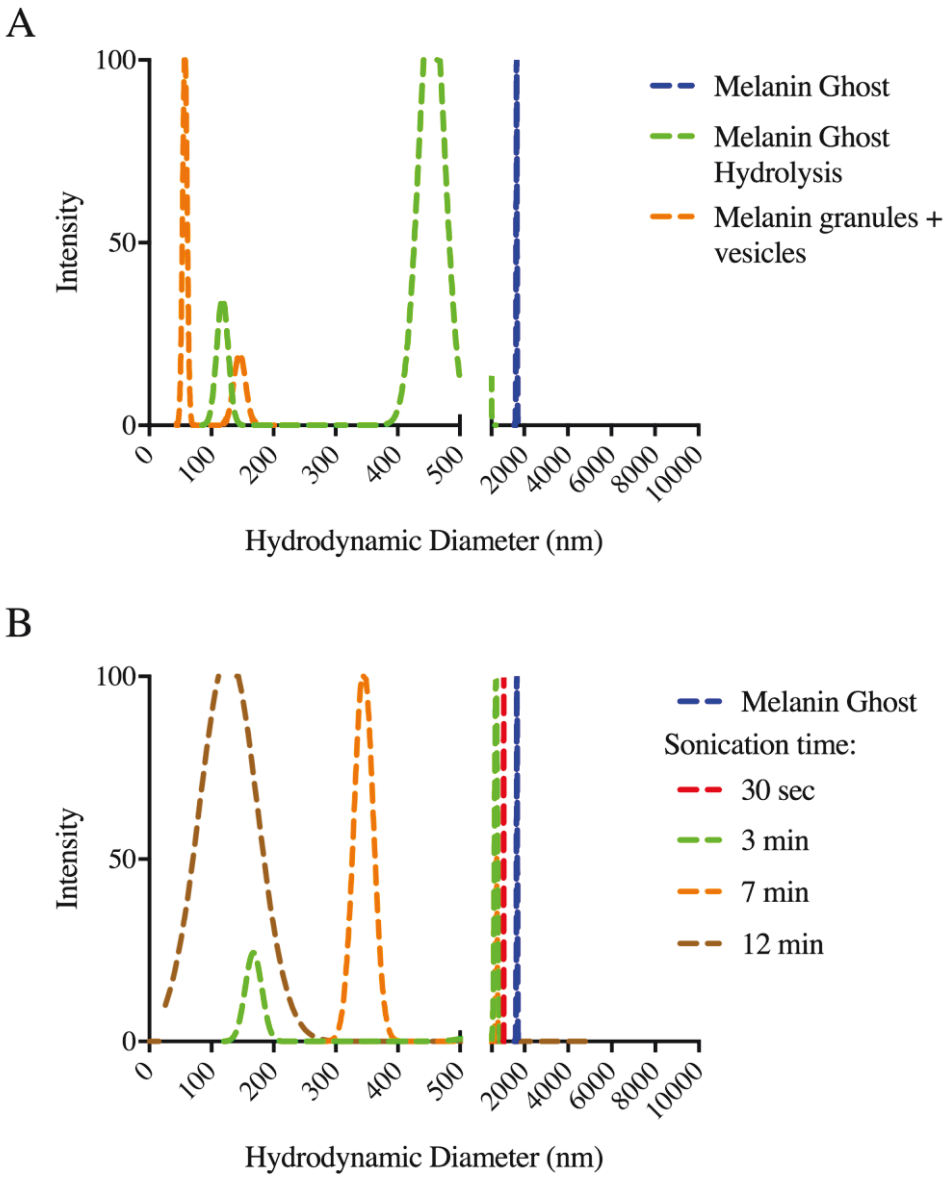

Figure 1.6: Breaking down the melanin ghosts. A. Representative data from two independent experiments depicting Size distribution of melanin ghosts (blue line), melanin ghosts upon extended hydrolysis (green line) and melanin granules + vesicles from H99 grown in MM with LDOPA (orange line). **B.** Ultrasonication of melanin ghosts breaks down the melanin isolated from the cell wall of H99 grown in MM at 12 minutes, data from a single experiment.

Discussion

In this study, we report the discovery of melanin granules secreted by *C. neoformans*. Melanin granules have a monotonic broadband absorption curve, are 40-80 nm in hydrodynamic size and aggregate depending on pH and salt concentration. Further analysis of the lipids and proteins associated with melanin granules will give us valuable insights in fungal melanogenesis and melanin structure. Future directions of this work include the characterization of secreted melanin granules by high-resolution EM, neutron scattering and NMR analysis to compare the structure and composition of melanin granules to the cell wall-associated melanin or 'melanin-ghosts'.

Melanin is an important virulence factor in many fungal pathogens. In filamentous fungi such as *A. niger*, the fungi synthesize the melanin precursor molecule called DHN. The importance of melanization of fungi in host-pathogen interaction was recently underscored by the discovery of a mammalian C-type lectin receptor that recognizes DHN-derived melanin of *A. niger* (19).

In mammalian systems, melanosomes are large organelles (~500 nm) that are the site of melanin synthesis, storage and transport. Pioneering EM studies classified four stages of melanogenesis in human melanocytes based on their morphology (20). Recently, the discovery of melanosomes in filamentous fungi, *Aspergillus niger* and *Fonsecaea pedrosoi* was reported (21, 22). In *A. niger*, the melanin synthesis enzymes localize in early endosomes that mature into multi-vesicular-bodies (MVBs) that is transported to the cell-membrane/cell-wall. While the study on *A. niger* suggested that the melanin granules are secreted, the authors did not show any evidence of secretion (21). Interestingly, the size of the melanin granules (40-80 nm) is similar to the size of vesicles, further suggesting that melanogenesis occurs in vesicles.

We also observed that the melanin granules secreted by *C. neoformans* have very low dispersity index (**Table 1.1**). This is consistent with the prevailing hypothesis that extracellular vesicles have low dispersity as the size of the secreted vesicles would depend on the curvature of the membrane and the permissibility of the cell wall of microbial organisms (23). Interestingly, the polydispersity of melanin granules increases with increasing salt concentration. While prior studies have shown that copper induced aggregation of synthetic melanin (24) and salts (divalent cations) cause vesicle fusion (17), we found that sodium and calcium cation induced aggregation of melanin granules. At higher concentrations, salts may disrupt the intermolecular interactions between water

and the hydrophobic and insoluble biopolymer melanin, causing the melanin granules to aggregate.

How *C. neoformans* forms its melanin coat is still unknown. The biosynthetic pathway of melanin formation in *C. neoformans* has not been elucidated. While, the isolation of cell-wall associated melanin as melanin 'ghosts' has allowed us to study the molecular interactions of melanin with cell wall and cell membrane (8), and the immunogenicity of melanin particles in murine models (6), the protocol for isolation is lengthy, and requires harsh treatment and conditions that must compromise the native structure of fungal melanin. Subcellular melanosome structures in *C. neoformans* have not yet been described, and the transcriptome studies comparing difference in melanized and non-melanized cells have yielded insignificant difference (25). In mammalian cells, sucrose density gradient centrifugation and free flow electrophoresis is used to separate melanosomes in various stages from subcellular fractions (26). The buoyant density of final stage mammalian melanosomes estimated by the density of the sucrose (1.8 M) the organelles equilibrate at is approximately 1.22-1.23 g/cc (26, 27). While our method of Optiprep density gradient ultracentrifugation suggests that the density of melanin granules is high (interface of 45%-35% Optiprep solution, ~1.195 g/cc-1.215 g/cc), it has been challenging to get an accurate measurement of density of melanin granules as the approximation relies on spectroscopic correlation (Optiprep absorbs at 340 nm in a concentration

dependent manner) and melanin absorbs all wavelengths of visible light (28). Furthermore, the granules have been determined to have a greater density than bead standards commonly used by Percoll density gradient centrifugation (<1.20 g/cc, data not shown).

The isolation and characterization of melanin granules will allow us to study the proteins and (potentially) lipids associated with melanin from *C. neoformans*. Since we believe that melanin granules arise from structures that were once vesicles, studying the proteins and lipids associated with secreted melanin granules will lead to identification of the subcellular machinery involved in melanogenesis and interactions required for melanin formation. Furthermore, the characterization of the melanin granules from *C. neoformans* mutants with 'leaky melanin' phenotype will help us understand the anchorage motifs of melanin on the cell-wall and cell membrane (13).

Previous studies have shown that mutant *C. neoformans* that do not produce the pigment cannot cause meningeal disease (29). Thus, studying the biosynthetic machinery involved in melanin formation could lead to the development of therapies that target fungal melanogenesis, and help control the dissemination of *C. neoformans* into the brain.

METHODS

Cell growth and culture conditions

Frozen stalks of *C. neoformans* H99 and Double KO Laccase mutant were inoculated into Sabouraud broth and incubated at 30°C for 48 hours, till the cultures reached stationary phase. The cells were counted using a hemocytometer. Approximately, 10^7 cells/ ml of were inoculated into minimal medium (10 mM $MgSO_4$, 29.3 mM KH_2PO_4, 13 mM glycine, 3 µM thiamine-HCl, and 15 mM dextrose with pH adjusted to 5.5) with and without L-DOPA (100 mM). As a control, *C. neoformans* were heat killed at 100°C for 10 minutes and streaked on Sabouraud agar plate to confirm complete cell death. MM (minimal medium) with or without L-DOPA, was inoculated with H99, Laccase mutant and heat-killed cells and incubated for 10 days at 37°C under continuous shaking at 180 RPM.

Isolation of extracellular vesicles (EVs)

The yeast cells were pelleted at 5,000 RPM Sorvall SLA rotor. The supernatant was filtered through a 0.22 µm Millipore filter, and pelleted at 100,000 *x g* for 1 hour at 4°C, with slow break in Beckman SW28 rotor. The pellet was suspended in 0.1X PBS and washed once. Next, the pellet was resuspended in approximately 500 µl of 0.1X PBS and stored in -80°C until further analysis.

Optiprep density gradient centrifugation

Optiprep solution (60%) dilutions were made in 10mM HEPES, 0.85% NaCl pH 7.4. The pellet was mixed with undiluted Optiprep to make a 45% solution that was layered at the bottom of the gradient. The gradient comprised of 45%, 35%, 30%, 25%, 15% and 10% layers in the ratio 0.4:3:3:2:1:1. The gradient was spun at 50,000 RPM for 10 hours in SW Ti55 rotor to allow the vesicles and granules to equilibrate at their respective densities. Ten equal volume fractions were collected from each tube.

Transmission Electron Microscopy

Negative staining was performed at the Johns Hopkins School of Medicine Microscopy Core. The fractions from Optiprep density gradients by adsorbing 10 µL of each fraction to glow-discharged 400 mesh ultra-thin carbon coated grids (EMS CF400-CU-UL) for two minutes, followed by 3 quick rinses of TBS and stained with 1% uranyl acetate with 0.05% Tylose. Grids were immediately observed with a Philips CM120 at 80 kV and images captured with an AMT XR80 high-resolution (16-bit) 8 Mpixel camera.

Measurement of hydrodynamic radius as a function of salt concentration

Dynamic light scattering (DLS) techniques gives an estimate of the size and heterogeneity of a sample by measuring the fluctuations of scattering light by particles in solution. Measurement of vesicle size by DLS was performed in a 90Plus/BI-MAS Particle Sizing analyzer (Brookhaven Instruments). To examine the colloidal properties as a function of salt concentration, 1M, 0.1 M, 0.01 M and 0.001 M solutions of Sodium Chloride (NaCl) and Calcium Chloride ($CaCl_2$) and 10X, 1X, 0.1X and 0.01X Phosphate Buffer Saline solutions were used to suspend 1 µl of vesicles/granules in 100 µl of the respective salt solution and an the average hydrodynamic diameter was obtained from 10 consecutive measurements.

Isolation of cell wall-associated melanin or melanin 'ghost'

Melanin was isolated from the cell wall of *C. neoformans* as detailed in (7). Briefly, cells were cultured in MM with L-DOPA for 14 days at 30°C, collected by centrifugation at 4000 RPM for 5 minutes and washed twice with PBS, the cell wall was lysed using lysing enzymes from *Trichoderma harzianum*, the cells were disrupted with a chaotropic salt guanidine thiocyanate, proteins and lipids removed by proteinase K digestion and Folch lipid extraction, boiled in 6N HCl for 2 hours, dialyzed and lyophilized.

Extended hydrolysis of melanin ghost

The supernatant from the acid hydrolysis step of the extraction of melanin from the cell wall of *C. neoformans* was collected to be analyzed. The melanin ghosts were suspended in fresh 6N HCl and allowed to sit for 5 days. The supernatant was collected and analyzed.

Sonication of melanin ghost

Five hundred microliters of a *melanin* ghost suspension in distilled water (1 mg/ ml) was sonicated with a horned sonicator at amplitude 5 for 12 minutes. Hydrodynamic radius of the suspension was measured at different time points using DLS as described above.

Chapter 2: The Buoyant Cell Density of *Cryptococcus neoformans* is Affected by Growth Conditions and Capsule Size

ABSTRACT

Cryptococcus neoformans is an environmental pathogenic fungus with a worldwide geographical distribution that is responsible for hundreds of thousands of human infections each year. During infection, the yeast form undergoes multiple morphological transformations impacting cell volume including capsular enlargement. To understand the factors that play a role in environmental dispersal of *C. neoformans* and *C. gattii* in this study, we evaluated the buoyant cell density of *Cryptococcus* by Percoll isopycnic gradients. We found differences in the buoyant cell density of strains belonging to *C. neoformans* and *C. gattii* species complexes, raising the possibility density influenced the environmental dispersal of different strains leading to a heterogeneous geographical distribution of the strains. The buoyant cell density of *C. neoformans* strains varied depending on growth conditions. In minimal medium, the cryptococcal capsule made a major contribution to the buoyant cell density such that cells with larger capsules had lower buoyant density than those with smaller capsules. Removing the capsule, both by chemical or mechanical methods, decreased the *C. neoformans* buoyant cell density. Melanization of the *C. neoformans* cell wall, which also contributes to virulence, produced a moderate but consistent increase in buoyant cell density. Finally, binding of the neutralizing monoclonal antibody IgG1 18b7 to the polysaccharide capsule resulted in a concentration-dependent increase in buoyant cell density suggesting that binding of capsular antibodies can affect cell density

via changes in capsule volume and/or hydration. The observation that the capsule reduces the buoyant density of *C. neoformans* cells suggests that it contributes to enhanced flotation in water, which could facilitate transport and dispersion of this organism in aqueous fluids

INTRODUCTION

Cryptococcus neoformans and *gattii* species complex are important fungal pathogens that can cause pulmonary and serious meningeal disease in humans (30). In the environment, *C. neoformans* is commonly found in soil associated with pigeon excreta, while *C. gattii* is most commonly found on trees (31, 32). Cryptococcal infection occurs via the respiratory tract where yeast particulates can colonize the lungs (33, 34). In immunocompromised patients, *C. neoformans* can readily disseminate from the lungs to other parts of the body, including the central nervous system by crossing the blood brain barrier. The dissemination of *C. neoformans* yeast cells from the lung to the brain is critical in the development of meningeal disease. The yeast cells undergo drastic morphological changes during this transition that aid its distribution and evasion from host immune mechanisms. For instance, yeast dimensions can range from 1 to 100 μm in diameter by increasing their cell body and/or growing a thick polysaccharide capsule at the cell wall surface in response to immediate environmental conditions.

The capsule is mostly composed of water (35), and has a porous matrix of branched heteropolysaccharides, mainly glucuronoxylomannan, that extends radially from the cell wall outpacing cell body growth (36). Capsule synthesis is induced under certain stressful conditions, and provides protection against host defense mechanisms by acting as a physical barrier, interfering with phagocytosis and sequestering Reactive Oxygen Species (ROS) and drugs (37, 38). The capsule is essential for causing disease and the target for both therapeutic and diagnostic strategies (39).

Melanin is another important virulence factor, such that strains that lack the ability to melanize cannot cause meningitis in mice (39). Melanin is formed by the polymerization of aromatic and/or phenolic compounds including L-DOPA, methyl-DOPA, epinephrine or norepinephrine (40). In the presence of catecholamine precursors, including L-DOPA found in the human brain, *Cryptococcus* melanizes its inner cell wall (5). Melanized *C. neoformans* cells are found in the environment (41) and during mammalian infection (42), suggesting an important role of the pigment in *C. neoformans* biology and pathogenesis. In fact, melanization protects cells against a variety of host immune mechanisms and antifungal drugs, as well as, against radiation, desiccation, ROS, and temperature stress (1, 43).

Both the polysaccharide capsule and melanin are very complex structures difficult to study and the application of biophysical methodologies provide new

insights into the physicochemical properties and biological functions of these major virulence factors (44). One such property that has not been studied in Cryptococcal biology is cellular density in liquid cultures and during infection, presumably a highly-regulated parameter that may reflects the physiological state of the cell under different conditions (45).

In the first century B.C., Roman writer Vitruvius describes a "Eureka" moment that the Greek polymath Archimedes had when, allegedly, he observed the displacement of water as he sat in a bathtub, which led him to establish the law of buoyancy (46, 47). In a biological context, Archimedes' law (law of buoyancy) can be applied to calculate the ratio of the absolute mass and volume of an organism which could determine whether it floats or sinks in a fluid of given density. In a continuous Percoll density gradient the cells of a given density equilibrate when they reach the same density inside the gradient during centrifugation, thus allowing us to estimate buoyant density of *C. neoformans* and *C. gattii* against bead standards of fixed density.

Buoyant density can be used for the separation of cell populations but the factors regulating buoyant cell density in microbiology remain understudied, despite the important role it can play in the migration and dissemination of microbial and mammalian cells in fluids. This could be because the buoyant cell density may depend on many biological and physical factors, which are often difficult to distinguish. Earlier studies found that the buoyant cell density in

bacteria may depend on the osmolality of the medium in which the cells are grown (48, 49), the encapsulation of bacteria by polysaccharide capsule (50) and the stage of cell cycle (51). Interestingly, strains of *Porphyromonas gingivalis* with different buoyant cell densities have different phagocytosis indexes, and vary in virulence, such that strains that had lower buoyant density and were highly hydrophilic surfaces were less susceptible to phagocytosis (52). Other studies have also reported a difference in buoyant density amongst different strains of mycobacteria and *Burkholderia* spp. (53, 54). In the context of eukaryotes, *Saccharomyces cerevisiae* buoyant cell density varies at different stages of cell cycle (55), and quiescent *S. cerevisiae* cell populations can be separated using density gradients in a stationary phase culture of the yeast (56). These methods have allowed us to create synchronous cultures without perturbation of the cell cycles. Intriguingly, the variation of buoyant density during cell cycle is not seen in some bacterial (*E. Coli*) and mammalian cell lines including Chinese Hamster Ovary cells and some murine cell lines (57, 58). A recent study measuring the cell density with high accuracy at a single cell level using microfluidic devices reported that the change in *S. serviciae* density at G1/S phase requires ATP derived energy, TOR function and an active cytoskeleton (59).

The buoyant cell density (also referred to as cell density) of *C. neoformans* and the factors that affect it have never been reported before to our knowledge. In this study, we use Percoll isopycnic gradients to study the effect of capsule

induction, antibody treatment, and melanization on the buoyant cell density of *C. neoformans*.

RESULTS

Comparison of *Cryptococcus neoformans* and *C. gattii* buoyant cell densities

The major pathogenic *Cryptococcus* spp. includes two species complexes known as *neoformans* and *gattii* (60). The *C. neoformans* species complex includes *C. neoformans* (serotype D), *C. grubii* (serotype A) and hybrids (serotype AD). The *C. gattii* species complex includes serotypes B and C. We found that the cell density varied consistently amongst different serotypes of *C. neoformans* and *C. gattii* species complex strains (**Figures 2.1, 2.2**). The cells were loaded onto a Percoll density gradient and the position at which the cells banded was compared to the position of colored bead standards of fixed density (**Figure 2.1A, 2.2A)** to estimate the density of the cells by linear correlation (**Figure 2.1B, 2.2B**.) The buoyant density of replicates has been plotted as a bar histogram that shows the variance of density between different strains of *C. neoformans* (**Figure 2.1C**) and *C. gattii*. (**Figure 2.2C**). There is large variance in some replicates (ATCC 2407, **Figure 2.1C**). In future directions, we want to confirm the growth curve of the strains used and confirm that all have reached stationary phase at 48 hours in minimal medium. To ascertain whether there was a

relationship between the density and cell dimension, we imaged the cells with an India-ink counterstain and calculated both the capsule and cell body size for *C. neoformans* (**Figure 2.1D**) and *C. gattii* (**Figure 2.2D**). However, we observed that the variation of buoyant density between stains cannot be explained by the variation in cell body and capsule size as there is no clear correlation between a strain that has larger cell capsule size and its buoyant density. The strains of *C. neoformans* and *C. gattii* have heterogeneous global distribution, and the mechanism of the dispersal are unknown (61, 62). Perhaps the varied density of the strains influences the differential dispersal of the fungal pathogen (see chapter 1 discussion).

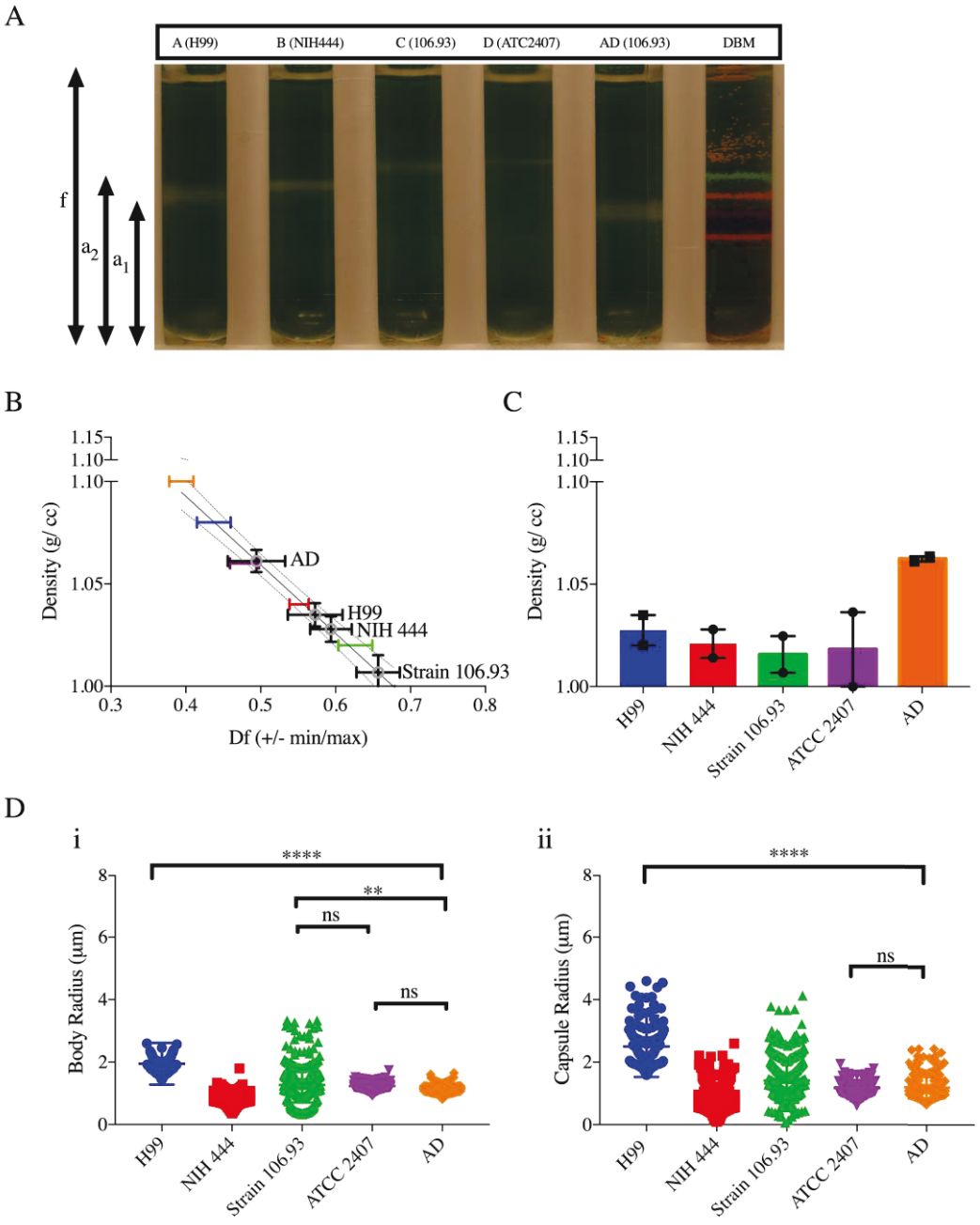

Figure 2.1: The buoyant cell density of *C. neoformans* serotypes.

A. Representative image of two independent Percoll density gradients comparing the buoyant density of *C. neoformans* Serotype A, B, C, D to density bead

markers (DBM). **B.** Representative data from two independent experiments depicting the line interpolation of the density factor (min, max) calculated by pixel areas as per the formulae ($f - a_1/f$, $f - a_2/f$). The df (min, max) values of the density marker beads are used to estimate the buoyant cell density of the cells ran in parallel. **C.** Histogram depicting the difference in buoyant cell density of different serotypes of *C. neoformans*. The experiment was performed twice, as indicated by the symbols on the bar graph, the error bar represents the range. **D.** Representative data of Capsule *i.* and cell body *ii.* radii of different strains.

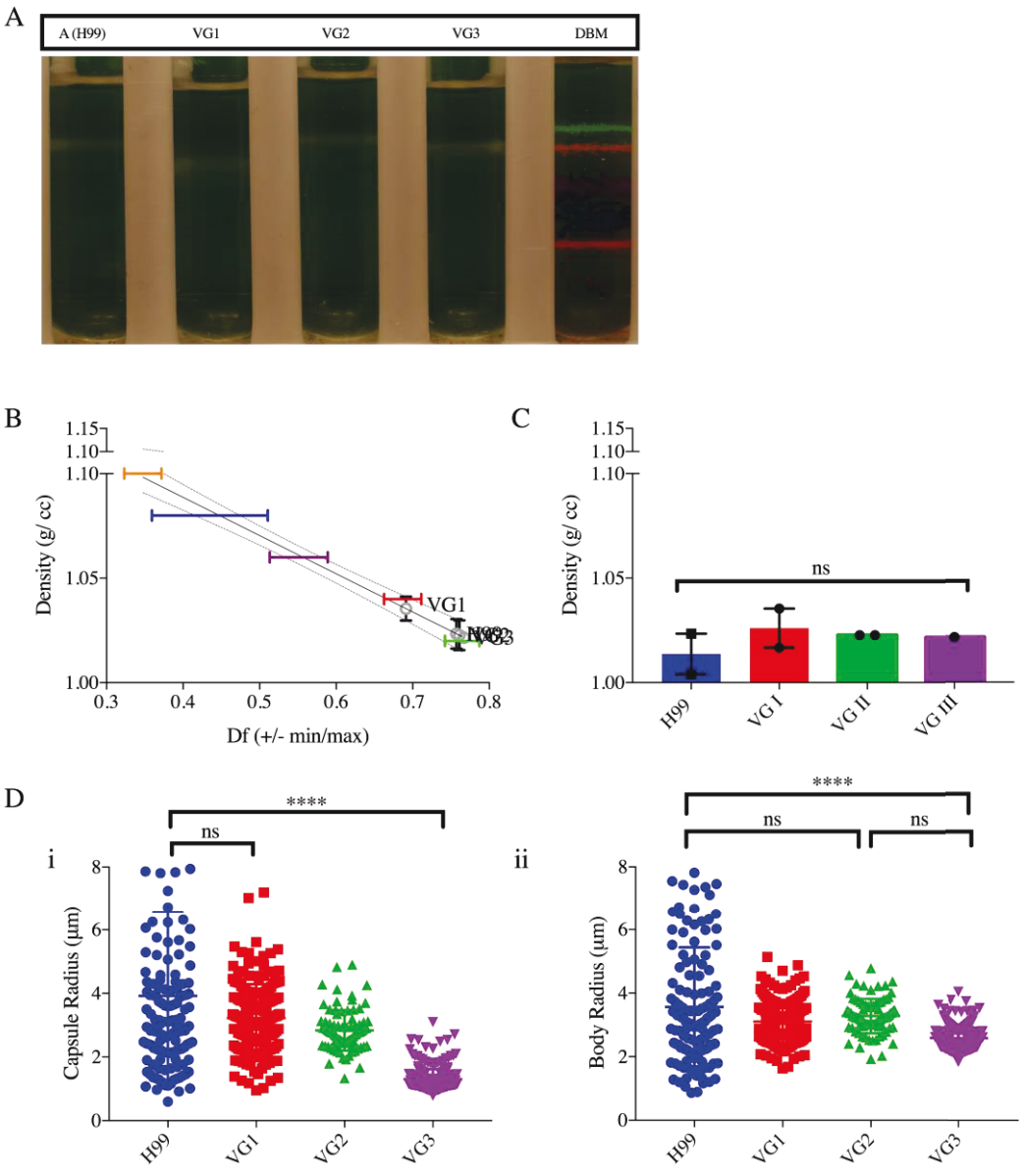

Figure 2.2: The buoyant cell density of *C. gattii* varies amongst different strains.

A. Representative image of independent Percoll density gradients comparing the density of different strains (Variant *Gattii* I, II and III) of *C. gattii* with *C. neoformans* H99 (Serotype A). **B.** Representative data from two independent

experiments depicting a line interpolation of the density factor with the buoyant densities of the bead standards as described in Figure 1. **C.** A histogram depicting the higher density of VG I in comparison to VG II, VG III and *C. neoformans* H99. Experiments were performed twice independently, as indicated by the data points on the histogram, except for VG III was performed once. The error bar represents the range. **D.** Representative data depicts *i.* the capsule radii and *ii.* the cell body radii of different strains of *C. gattii* and *C. neoformans* H99.

Effect of capsule induction on *C. neoformans* buoyant cell density

Yeast cells with large capsules can be isolated from lungs of mice where the capsule serves a protective role by interfering with phagocytosis and quenching microbicidal compounds (63). In vitro, the capsule is induced in stress conditions such as nutrient starvation medium (64). We found that cells grown in minimal medium (MM) had significantly lower density (**Figure 2.3A-C**) in comparison to cells grown in nutrient rich conditions (Sabouraud broth) where the capsule was much smaller (**Figure 2.3D i**). Acapsular strains (*cap59*) had a significantly higher density than encapsulated cells with the same genetic background. Furthermore, we observed no significant differences in the density of acapsular mutants grown in minimal versus rich medium, confirming the contribution of the polysaccharide capsule in determining the cell density in response to different nutrient conditions. To examine other factors that may affect the buoyancy of cells grown in different conditions, we quantified the neutral

lipid content using fluorescence microscopy since lipids have lower buoyancy than water. For cells grown in rich medium, we observed higher lipid content by quantification of BODIPY neutral lipid staining (**Figure 2.3E ii**). We also observed small dense vacuoles/vesicles in cells grown in Sab, when compared to cells grown in MM (**Figure 2.3E i**). The clear difference in capsule radii of cells grown in minimal medium and rich medium suggests that the capsule plays a more prominent role in determining the cell density than lipid content.

Previous studies have studied the molecular composition of the *C. neoformans* capsule by removing the polysaccharide from the cell surface by DMSO extraction and gamma irradiation induced capsule shedding (65). To confirm the effects of the capsule to buoyant cell density, encapsulated H99 cells were treated with gamma radiation and DMSO to remove capsular material (**Figure 2.4**). We observed an increase in cell density when the capsule was removed by DMSO extraction, although the difference was not statistically significant ($p=0.049$). The decrease in buoyant density was more dramatic following irradiation and a less prominent after DMSO treatment (**Figure 2.4A-C)** consistent with the fact that the former treatment is more effective in removing the capsule (**Figure 2.4D**). Thus, the polysaccharide capsule, an essential virulence factor, also influences the cell density. Furthermore, buoyant density may be used for the separation of different populations of yeast cells (56), to

characterize *C. neoformans* mutants with capsular defects (66) and for the isolation of the titan cells (67).

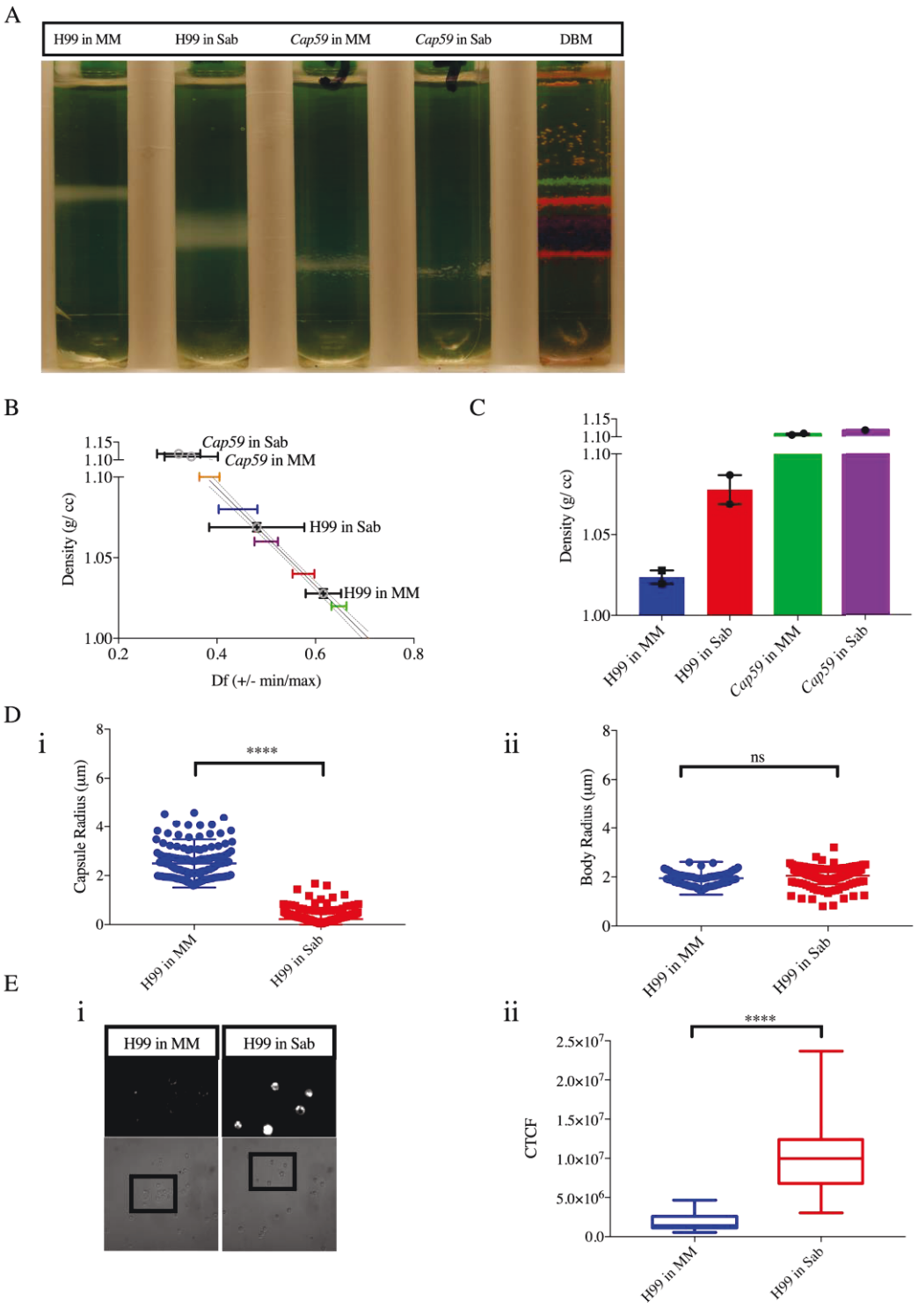
A
H99 in MM
H99 in Sab
Cap59 in MM
Cap59 in Sab
DBM
B
Cap59 in Sab
Cap59 in MM
H99 in Sab
H99 in MM
Density (g/ cc)
Df (+/- min/max)
C
Density (g/ cc)
H99 in MM
H99 in Sab
Cap59 in MM
Cap59 in Sab
D
i
Capsule Radius (µm)
****
H99 in MM
H99 in Sab
ii
Body Radius (µm)
ns
H99 in MM
H99 in Sab
E
i
H99 in MM
H99 in Sab
ii
CTCF
****
H99 in MM
H99 in Sab

Figure 2.3: Induction of capsule synthesis decreases C. neoformans cell buoyant density.

A. Representative image of independent Percoll density gradients showing the density of *C. neoformans* H99 juxtaposed with acapsular mutant *Cap59*, both grown in rich medium (Sab), minimal medium (MM). **B.** Representative data from two independent experiments depicting a line interpolation of the density factor with the buoyant densities of the bead standards to calculate the buoyant cell densities of the gradients run in parallel. **C.** Histogram depicting a decrease in the range of buoyant cell density in H99 cells grown in MM, when compared to Sab, possibly due to capsule induction. *Cap59* mutant are significantly denser than normal H99 cells grown in MM. Experiments were performed in replicates independently, as indicated by the data points on the histogram, except for *Cap59* in Sab was performed once as indicated by the symbols on the bar graph, the error bar represents the range. **D.** Representative data depicts *i.* the capsule radii and *ii.* the cell body radii of different strains *C. neoformans* H99 grown in different medium conditions (MM, Sab). The size of acapsular mutant cap59 mutant was not quantified because the yeast cells tend to clump. **E.** *i* Bright field images with insets of fluorescence microscopy (five fields at equal exposures, 20X) to quantify corrected total cell fluorescence (CTFT), *ii* compares the intracellular neutral lipid content (BODIPY binding) in *C. neoformans* grown in nutrient rich and starvation conditions. Data from a single experiment.

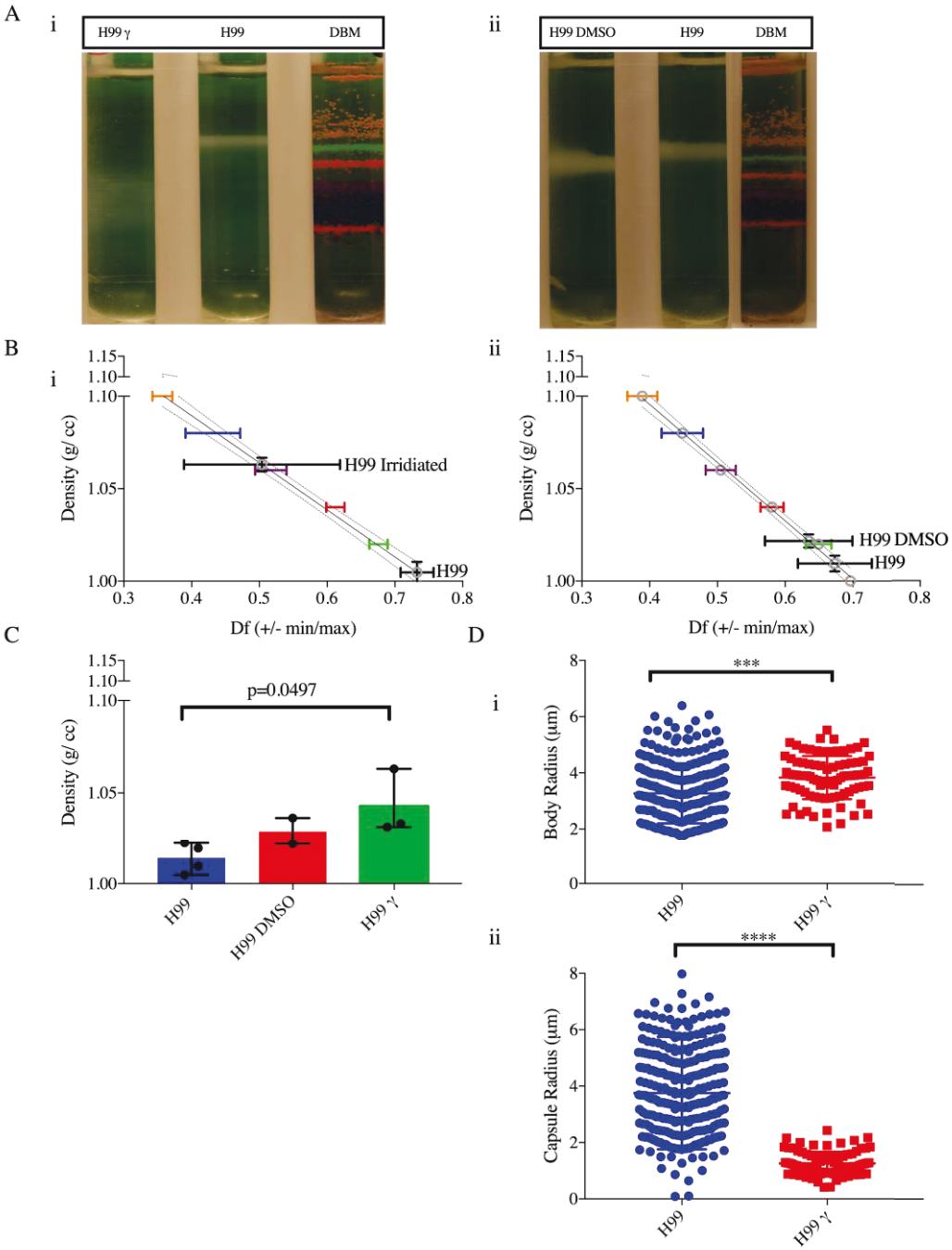

Figure 2.4: Removal of *C. neoformans* increases the buoyant cell density. A. *i* Representative image of three independent Percoll density gradients comparing the buoyant cell densities of irradiated (γ) and non-irradiated *C. neoformans*

(H99) with a standard of colored uniform density beads. *ii* Representative image of two independent Percoll density gradients of encapsulated *C. neoformans* H99 strains before and after DMSO extraction. **B.** *i, ii* Representative data from independent experiments depicting a line interpolation of the density factor (df) with the buoyant densities of the bead standards, to calculate the buoyant cell densities of *C. neoformans* before and after extraction of the capsule, run in parallel. **C.** A histogram depicting buoyant density of *C. neoformans* before and after capsule extraction by γ rays and DMSO. The irradiation experiment was performed independently thrice, and the capsular extraction by DMSO twice, as indicated by the symbols on the bar graph, the error bar represents the range. **D.** Representative data depicts *i.* the capsule radii and *ii.* the cell body radii of *C. neoformans* before and after gamma irradiation capsule shedding.

Antibody binding to the capsule affects *C. neoformans* buoyant density

Antibodies against the *C. neoformans* capsule can protect mice against Cryptococcal infection by several mechanisms ranging from immobilization and opsonization of yeast cells, to directly altering yeast physiology making it more susceptible to antimicrobial stressors (68) . The direct antimicrobial function of such protective capsular antibodies may be associated to their ability to change capsule structure and viscoelastic properties (69). The binding of antibodies to the capsules alters the rate of cell division and budding, and also inhibit GXM release (69, 70). The alteration of mechanical properties of the capsule, such as stiffness is thought to occur due to antibody mediated antigen aggregation, and

crosslinking of polysaccharide molecules which is supported by data from light scattering experiments (69). Since our study found that the polysaccharide capsule is a major contributor to cell density of *C. neoformans*, and antibody binding alters the biomechanical properties of the capsule we were interested in studying the effect of antibody binding on buoyant cell density of the yeast. We observed that the antibody 18B7 (71) tends to increase the cell density in a concentration-dependent manner, although this difference is not statistically significant, while another protective antibody IgG1 E1 (72), despite effective capsular binding, does not seem to have an effect on the buoyant cell density (**Figure 2.5C**). Understanding of antibody mediated immunity is ever expanding with renewed efforts to understand the mechanisms of their protection (73). The effect of 18B7 on the density of *C. neoformans* may lead to novel insights into the protective function of antibody.

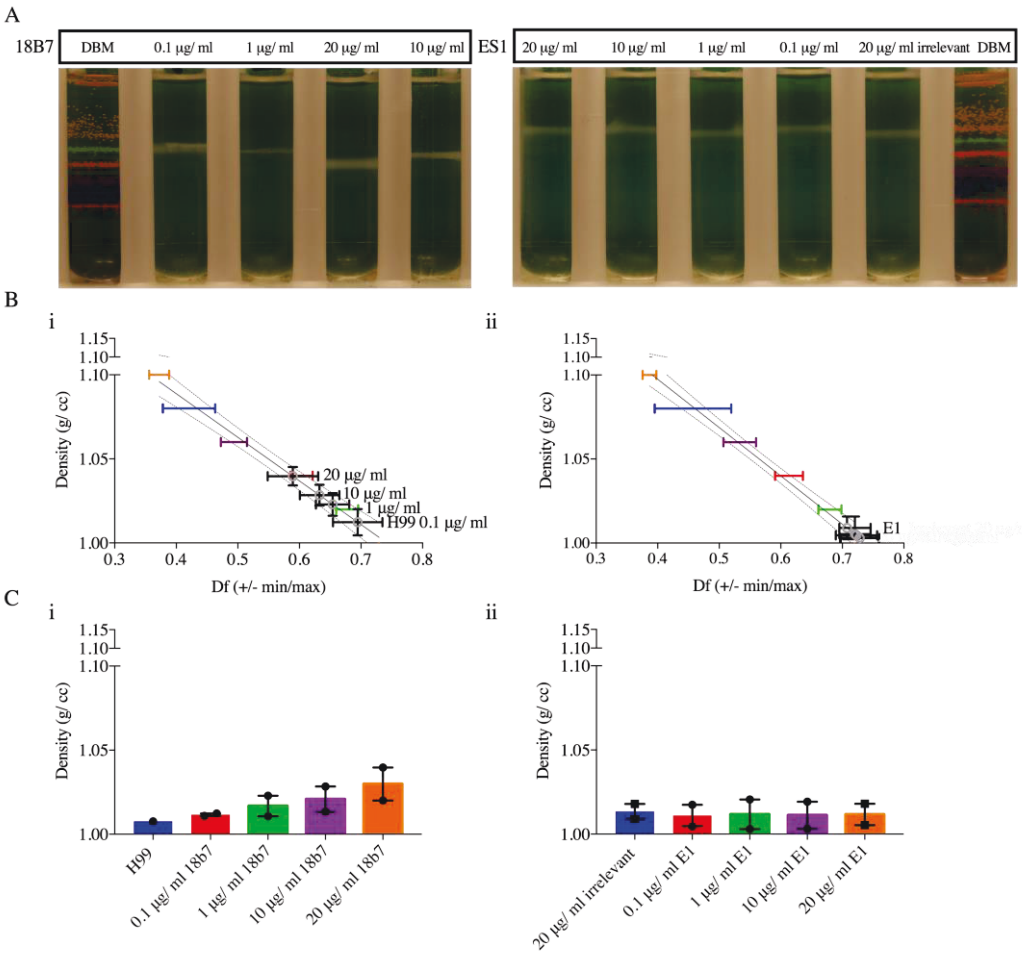

Figure 2.5: Effect of capsule binding antibody on *C. neoformans* buoyant density. **A.** Representative image of independent Percoll Density Gradient of H99 strain encapsulated *C. neoformans* cells incubated (1 hour, at 30°C) at different concentrations of antibody 18B7, E1 and highest concentration of irrelevant antibody (IgG2 anti rat) which has been compared density bead standards ranging from low to high density. **B.** Representative data from two independent experiments depicting a line interpolation of the density factor with the buoyant density of the cells treated with *i.* 18B7 *ii.* E1 antibodies. **C.** Histogram of the interpolated buoyant densities of H99 *C. neoformans* incubated

with 18B7 antibody showing a concentration dependent increases while those incubated with E1 antibody shows a slight decrease in the buoyant cell density, which seems to be independent of the concentration, when compared to the buoyant cell density of *C. neoformans* incubated with an irrelevant antibody. The experiment was performed independently twice, as indicated by the symbols on the bar graph, the error bar represents the range.

Melanization increases *C. neoformans* buoyant density

Comparison of melanized and non-melanized H99 *C. neoformans* cells demonstrated that melanization was associated with a slight increase on cell density (**Figure 2.6A-C)**. Since the increase in the buoyant density was small, and melanized culture (black) can easily be distinguished visually from non-melanized cultures (white), we mixed the melanized and non-melanized cells in 1:1 ratio before loading the samples onto the density gradient (**Figure 2.6A-C**). We observed that non-melanized *C. neoformans* cells displayed a range of density that overlapped with the range of density estimated for melanized cells, although melanized cells tend to have slightly higher density when compared to non-melanized cells. Melanin ghosts had much greater density than cells, estimated to be > 1.1 g/cc. (data not shown). Despite this much greater density cellular melanization had only a small effect on cell buoyant density given that melanin comprises approximately only 15.4% mass of melanized cells (7). Note that

melanized cells also exhibit smaller capsules (Figure **2.6D**), which may also synergize with melanin to decrease buoyant cell density.

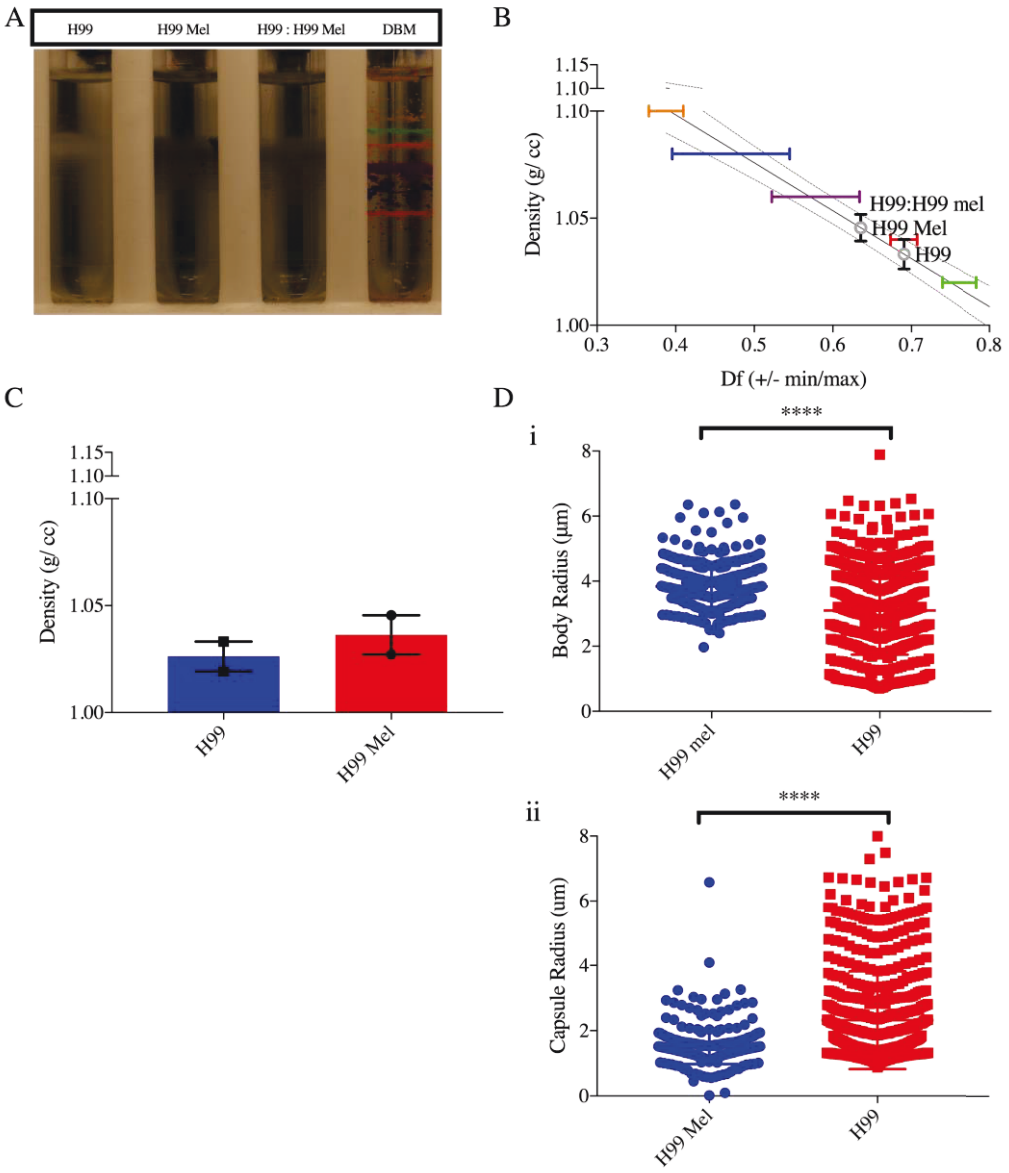

Figure 2.6: Effect of Melanization on *C. neoformans* buoyant cell density. A. Representative Percoll density gradients comparing the density of H99 in MM, H99 in MM with L-DOPA (mel) and a 1:1 mixture of the cells. The white cells

(H99) band slightly above the melanized black cells (mel) as can be seen by the gradient that contains the mixture. **B.** Representative data from two independent experiments depicting a line interpolation of the density factor with the buoyant densities of the bead standards, to calculate the buoyant cell densities of the gradients run in parallel. **C.** A histogram depicting an increase in buoyant cell density of melanized *C. neoformans*, which is not significant. The experiment was performed independently twice, as indicated by the symbols on the bar graph, the error bar represents the range. **D.** Representative data depicts *i.* the capsule radii and *ii.* the cell body radii of melanized and non-melanized *C. neoformans*.

Other conditions that have no significant effect on *C. neoformans* buoyant cell density

Treatment of H99 *C. neoformans* with complement, different concentrations of salts to induce osmotic stress, 6D2 antibody to melanin and incubation in lipid rich medium had no significant impact on the buoyant cell density of *C. neoformans* (data not shown, experiments were performed once).

DISCUSSIONS

In this study, we characterized the buoyant cell density of *C. neoformans* and *C. gattii* in different conditions, seeking to understand the factors that contribute to the buoyant density. We report minor differences in buoyant densities between serotypes of the cryptococcal species complex that reflects the

genomic and antigenic differences between strains as an important biophysical parameter. Our results also suggest that the capsule plays a major role in decreasing the buoyant cell density of the yeast such that the density is close to that of water. Meanwhile, melanization increases the density slightly. Changes in buoyancy could influence the transmission of the yeast in the environment, and dissemination of the fungal pathogen during infection. Interestingly, the binding of certain capsular antibodies (18B7) seems to increase the cell density. While we see definite trends in our data, in our future work we want to confirm these results with more replicates. The total lipid content of cells can also be determined by Thin Layer Chromatography, which will allow us to compare the extracted lipid content from equal number of cells grown in nutrient rich and starvation conditions. We expect to find that the cells grown in rich media (Sab) would a higher lipid content than cells grown in minimal medium.

The buoyant density of a microbe is a fundamental biophysical property that influences its behavior in aqueous fluids. Depending on its density, a microbe could remain suspended in a fluid or settle to the bottom. Amongst other factors, this could influence the microbe's access to nutrients, sunlight and oxygen. Thus, it is not surprising that marine and freshwater unicellular organisms including phytoplankton, regulate their cell density via mechanisms that involve the synthesis and storage of gas vacuoles, polysaccharide mucilage sheaths, and glycogen (74). Interestingly, the polysaccharide mucilage sheath of

these bacteria has been characterized as an important factor that decreases the density of the cell to just below the density of water (75). Our data demonstrates that the cryptococcal capsules both serves a similar function by increasing the volume of the yeast cell without significantly increasing its mass and thereby decreasing the density.

Cryptococcus gattii have been isolated from marine and fresh water environments (76, 77). We found that the density of encapsulated *C. neoformans* is close to that of water (1.00 g/cc). A quantitative parameter used to determine how fast a population of microbial cells sinks in a fluid of given density is the settling velocity, which is calculated by the Stoke's law and depends on the buoyant density and the size (diameter) for a spherical object such as a yeast cell (74, 78). In marine bacteria, low cell density (< 1.064 g/cc) correlates with low settling velocity as calculated by Stoke's law (79). The variable size of *C. neoformans* grown in minimal medium (3-16 μm) and the density (< 1.05 g/cc) we observed during nutrient starvation conditions in an aqueous environment suggests that the settling velocity of *C. neoformans* would be similarly low. More importantly, the encapsulated *C. neoformans* cells would have a lower settling velocity when compared to similar-sized cells that have no capsule due to the decrease in density.

We hypothesize that this may influence mobility allowing the yeast to flow horizontally in aqueous environment to access (80) nutrients, oxygen and

disperse the pathogen (81). For instance, a study found that a *C. gattii* clinical isolate survived well in filtered ocean water, distilled water and saline water (up-to 10% of initial inoculum) at room temperature up to 94 days (82). The resistance of *Cryptococcus* to different levels of osmotic stress is consistent with our observations that high salt concentrations do not alter the cell density. Thus, in the context of environmental fungal pathogens *C. neoformans* and *gattii*, the cell density could play an important role in determining the dispersal of the yeast in the environment and affect its ability to infect a wide range of hosts. Estimating the settling velocity of microbial cells in aqueous fluids will add weight to the hypothesis that the buoyant density of *C. neoformans* and *C. gattii* influences environmental dispersal. We are currently optimizing a method to calculate the settling velocity of *C. neoformans* and *C. gattii*.

C. neoformans infects lungs via infectious propagules and after infection can reside in granulomas. In immunocompetent individuals, the immune system is able to control this yeast infection. However, if the host is immunocompromised, the yeast can disseminate to the brain where it causes life-threatening meningitis. Presumably, this multistep process requires the pathogen to travel into the draining lymph node and into fluidic blood and lymph systems to survive and grow outside the lungs. Could the density of *C. neoformans* is likely to influence the movement of the yeast cells in these fluids? Interestingly two of the major virulence factors, melanin (increases) and capsule (decreases), affect the cell

density of *C. neoformans,* although the effect of melanin was small effect relative to that of the capsule and any contribution of pigment was obscured by smaller capsules. Murine models of infections have shown that host defense mechanism induce larger capsules in *C. neoformans* found in the lungs, with an approximate size of 20.0 ± 6.1 μm (83). This can also be replicated in-vitro by growing the cells in nutrient starvation conditions (64). We found that the presence of the capsule, and its size could play a role in regulating the cell density of the yeast. This could potentially affect the phagocytosis of the pathogen and the way the yeast is disseminated in vivo. Interestingly, the *C. neoformans* isolated from the brain is often smaller and has a smaller capsule (83). The enzyme laccase is a polyphenol oxidase that oxidizes melanin precursors such as L-DOPA to form melanin. *C. neoformans* that are deficient in laccase are unable to melanize and are not able to disseminate from the pulmonary tissues to the brain (84) but intravenously injected mutant yeasts are able to survive and cause infection in the brain, suggesting a role of laccase or melanin in facilitating lung escape. Although the contribution of melanin to overall cell density is small, it is conceivable that it could influence dissemination of the yeast in some circumstances, especially when capsules are small.

Capsular antibodies can mediate protection against *C. neoformans* (71). These antibodies bind to the capsule and promote phagocytosis by innate immune cells. Previous studies have shown that capsular antibodies alter the rigidity

(Young's modulus) and structure of the capsule (69). Antibody binding also causes a change in the hydration state of the PS capsule (85). We found that the capsule-binding antibody 18B7 increases the cell density of the cells in a concentration-dependent manner. Although the mechanism for antibody mediated reduction in density is unknown, it is likely that changes in capsule structure resulting from antibody mediated cross-linking of polysaccharide molecules that affect capsule hydration levels and volume, as has been previously described (69, 85). Interestingly, the observed increase in density due antibody 18B7 was not seen in another opsonic capsular antibody (E1). The finding that antibody 18B7 tended to increase density, together with promoting agglutination (71, 86), could conceivably reduce transportability in body fluids and thus effect dissemination. However, we currently lack the mechanistic understanding of the effects of a pathogen's buoyancy on its movement in viscous fluids such as blood. Thus, the influence of density of a pathogen in dissemination during the course of infection remains to be explored.

In summary, we determined the density of *C. neoformans* grown in minimal medium to be slightly greater than that of water. The presence of a capsule reduced the density such that it approached that of water. Hence, the capsule, by reducing density, also reduces the settling velocity of *C. neoformans* in aqueous solutions, which could favor environmental dispersal. The establishment of *C. gattii* in the Pacific Northwest is reported to have occurred

relatively recently (87). Although the means by which this organism reached North America are unknown the fact that it has been recovered from marine environments (82) together with our finding of a low density of yeast cells indicating a propensity of the pathogen to float suggest that sea currents could have transported *C. gattii* between continents. The observation that the polysaccharide capsule makes a large contribution to reducing density suggests a new role for this structure in the environment as an aid to cell dispersal and transport in aqueous fluids.

MATERIALS AND METHODS

Yeast culture

Frozen stocks of *C. neoformans* and *gattii* strains were inoculated into Sabouraud agar rich medium (pH adjusted to 7.4) at 30°C for 48 hours. Yeast cultures of *C. neoformans* included Serotype A strain H99 (American Type Culture Collection (ATCC) 208821), Serotype B strains NIH 191 and NIH 444 (ATCC 32609), Serotype C strain 106.93, Serotype strains D ATCC 24067 and B-3501 (ATCC 34873), and Serotype AD strain MAS92-203 and *Cryptococcus gattii* included variants I, II and III. Acapsular mutants from *Cryptococcus neoformans* cultured included Cap59 (Background H99, serotype A) and Caps67 (Background B3501, Serotype B). Approximately 10^6 cells from the stationary phase cultures in Sabouraud broth were washed twice in Minimal Medium (10 mM $MgSO_4$, 29.3 mM KH_2PO_4, 13 mM glycine, 3 μM thiamine-HCl, and 15 mM dextrose with pH adjusted to 5.5). The washed cells were inoculated into Minimal Medium (MM) for capsule induction, MM with L-DOPA (100 mM) to induce melanization, and Sabouraud broth for providing rich medium conditions. Cells were incubated at 37°C for 48 hours, rotating at 180 RPM. Cells were washed twice with sterile PBS (Phosphate Buffer Saline), centrifuging them for 5 minutes at 4700 x *g*. Cells were counted using a hemocytometer, and dilutions were made to obtain 1 X 10^7

cells in PBS. The cells were then loaded onto Percoll Density gradients with or without treatments to test the effect of different conditions on the buoyant cell density.

Density gradient centrifugation

Percoll is a non-toxic and isotonic alternative to the commonly used sucrose gradient, and is composed of polyvinylpyrrolidone coated colloidal silica particles (88). Percoll has found applications for separation of mammalian blood, tumor, immune and endothelial cells, and microbial cells due to its ability to form reproducible self-generated continuous gradients (89). Stock Isotonic Percoll (SIP) was obtained by added 1 part of 1.5 M NaCl to 9 parts of Percoll. The working solution of 70% (v/v) was obtained by diluting SIP with 0.15 M NaCl, to a final density of 1.0914 g/ml. Three milliliters of this solution were loaded into polycarbonate ultracentrifuge tubes (13 X 51 mm). Approximately, 10^7 cells were pelleted at 4700 x *g* and over layered directly or after treatment. All gradients were run in parallel with a standard tube.

For the preparation of the standard tube, 10 µl of each uniform density bead standard (Cospheric DMB kit) including light orange (ORGPMS-1.00 250-300um, density 1.00 g/cc), fluorescent green (1.02 g/cc), florescent orange (1.04

g/cc), florescent violet (1.06 g/cc), dark blue (1.08) and florescent red (1.099 g/cc), was loaded and mixed with the Percoll.

By varying time and speed of centrifugation, it was found that the most optimal separation of the density gradient beads, which was taken as an indication for the most optimal continuous density gradient formed, occurred at 40,000 RPM for 30 minutes (acceleration 9, deceleration 0), in TLA 100.3 fixed angle rotor in Optima TLX tabletop ultracentrifuge.

Buoyant cell density estimation

First, the images of the density gradient were taken under uniform light and shadow conditions using Nikon D3000 DSLR, Auto settings. Next, pixel area measurements were taken from the bottom of the tube, to the area at the beginning of each band (a1), ranging to the end of each band (a2), to the upper meniscus of the tube (f). The density factor, $D_f\ (min,\ max)$, and the average along with the standard deviation was computed on Microsoft Xcel according to the following formulae,

$$D_f(min, max) = \left\{\left(\frac{f - a_1}{f}\right), \left(\frac{f - a_2}{f}\right)\right\}$$

A standard curve was derived, where D_f (min, max) and buoyant density (g/l) of the density marker beads were computed by linear regression. A 95% confidence

interval was used to interpolate the mean density of sample cells, around a standard deviation, run in parallel with the uniform density bead standards.

Although, the results from different Percoll gradient runs follow the same trend, the exact density values can vary considerably. This can be attributed to pipetting errors or errors in measurement of density factor.

Gamma irradiation of cells for capsule removal

Approximately 10^9 cells of melanized and non-melanized cells were plated on a 24-well plate. The cells were irradiated to a total dose of 1500 Gy, using Shepherd Mark 1 at the SKCCC Experimental Irradiator Core at Johns Hopkins University Sidney Kimmel Comprehensive Cancer Center. Cells were washed twice in PBS and approximately 10^7 cells were pelleted at 4700 x *g* and loaded onto the gradient.

DMSO Extraction of *C. neoformans* capsule

Approximately 10^7 cells were incubated in 15 ml of DMSO at 30°C for 30 minutes to allow capsule extraction. The cells were washed thrice in 1X PBS, pelleted and loaded onto the Percoll density gradient.

Antibody Coating of *C. neoformans* capsule

Purified antibodies, 18B7 and E1 (kindly provided by the Dromer's laboratory), were obtained from stock solutions kept at 4°C. The antibodies were serially diluted in PBS to concentrations of 20µg, 10µg, 1 µg and 0.1 µg/ml. A pellet of 10^7 cells was suspended with 1 ml of each Ab solution in Eppendorf tubes, vortexed and incubated at 28°C on a rotating mixer, for 1 hour.

***C. neoformans* melanization**

Frozen stalks of *C. neoformans* H99 was inoculated into Sabouraud broth and incubated at 30°C for 48 hours, till the cultures reached stationary phase. The cells were counted using a hemocytometer. 10^6 cells/ml of were inoculated into minimal medium (10 mM MgSO4, 29.3 mM KH2PO4, 13 mM glycine, 3 µM thiamine-HCl, and 15 mM dextrose with pH adjusted to 5.5) with and without L-DOPA (100 mM). The cells were cultured for 10 days at 30°C rotating at 180 RPM. The cells were washed twice in PBS, and 10^7 cells were pelleted at 47000 x *g* loaded of melanized, non-melanized and 1:1 mixture of the cells was loaded onto the gradient. Melanin ghosts were prepared as described (7).

Mouse complement deposition in *C. neoformans*

Frozen stocks of guinea pig complement (1 mg/ml) were thawed. 50% (500 g/ml), 20%, 10% and 1% dilutions with PBS was added a pellet of 10^7 cells. The cells were incubated with complement for approximately 1 hour at 28°C in a rotating-mixer.

Providing *C. neoformans* with osmotic stress

C. neoformans (approximately 10^8 cells) were incubated with 1 ml of 10X PBS, 1X PBS, 0.1X PBS and ultrapure distilled water (MilliQ) for 2 hours in 30 rotating-mixer at 28°C.

Visualization and estimation of intracellular lipid content

C. neoformans cells were grown for the indicated times and then stained with BODIPY 493/503 (1:200) for 30 min and 0.01% Uvitex 2B for 10 min at room temperature and washed twice with PBS prior to visualization by microscopy. The lipid content was estimated by calculating the corrected total cell fluorescence: CTCF = Integrated Density – (Area of selected cell × Mean fluorescence of background readings).

Cell imaging and yeast size measurements

The cells were visualized and imaged with India Ink negative staining under Olympus AX70 Microscope at 20X magnification. The capsule and cell body size was estimated using an automated measurement Python software (90).

Statistical analysis

All statistical analysis was performed on GraphPad Prism 7.0 software. The density of cells was estimated by using making a standard curve from beads of different densities using linear regression to estimate the unknown values of a given sample with a 95% confidence interval. One-way ANOVA statistics using a Kruskall-Wallis non-parametric test was used to compare the differences among groups with a 95% confidence interval in all experiments. Student t-test was used when only two groups were compared.

FINAL THOUGHTS

Buoyancy is a concept of historical importance. The question is why? If we are to believe the fable of Archimedes, the king wanted to know if his crown was made of authentic or counterfeit gold. Specific gravity, the ratio of the density of a substance to that of a standard, was an easily measurable physical parameter that allowed Archimedes to distinguish pure gold from other metals.

Today, we have developed tools to exploit the intrinsic property of buoyant density to separate cells, organelles, extracellular vesicles, proteins, lipids and DNA. As our lab started investigating the buoyant density of *C. neoformans*, a prominent question emerged. Is the buoyant density an incidental consequence of the biomolecular assemblies and thermodynamic stability of a cell? Or is it a highly regulated biophysical parameter that plays a role in cell survival?

In the context of *C. neoformans*, studies on Titan cells (>10 μm) have shown the role of simple physical parameters like cell size in the pathogenesis. Could the buoyant density of other microbial pathogens also play a role in pathogenesis? While we believe this is an important question to ask, it is a challenging question to answer. Our study shows that the capsule plays an important role in determining the cell density of *C. neoformans*. However, the capsule is also an essential virulence factor that acts as a physical barrier and protects the yeast from host defense mechanisms like ROS, antifungals etc. This

makes it difficult to tease apart the capsule's effect on buoyant density from its other immunosuppressive roles during infection.

Possibly due to these limitations, cell density of microbial organisms remains understudied. More recently the development of microfluidic systems have made it possible to measure single cell density (45, 91) and advanced the field by allowing us to measure the biophysical parameter with high accuracy (0.001 g/ml).

In the emerging field of extracellular vesicles, the low buoyancy of extracellular vesicles (>1.1 g/cc) allows us to separate them from other components present in the medium, including secreted proteins, protein aggregates and cell debris (92). The high buoyant density of melanin granules secreted by *C. neoformans* allowed us to separate them from the less dense extracellular vesicles. Thus, the biophysical property (density) of the melanin granules has allowed us to isolate secreted melanin from a microorganism for the very first time.

The supramolecular assembly of DOPA melanin in biological systems remains a mystery to this date. One of the major challenges has been the limitations in isolating native melanin granules from vertebrates and scuttle-fish, organisms whose melanin structures have been most extensively studied (93). In these organisms, melanin granules occur in agglomerated structures, and using mechanical or chemical means to disrupt the intermolecular forces that hold the

granules together compromises the native structure (94). Thus, studying the biophysical and structural characteristics of melanin granules in its native form secreted by *C. neoformans* will provide valuable insights to the melanin field.

Furthermore, the characterization melanin granules from *C. neoformans* may find a wide range of applications. For instance, the IgM 6D2, an antibody that has been made against "melanin-ghosts" isolated from *C. neoformans* (95) has proven to be a useful tool in melanin studies and in the development of immunotherapies. Given their ease of isolation in native state, studies on the immunogenicity of secreted melanin granules may give us an opportunity to create more effective antibodies against this cryptococcal antigen. Furthermore, fungal systems provide scalable opportunities to optimize the production of melanin granules/nanoparticles that already find a wide range of application in radioprotection during immunotherapy (96), iron chelation therapy (97) and much more.

REFRENCES

1. Cordero RJB, Casadevall A. 2017. Functions of fungal melanin beyond virulence. Fungal Biol Rev 31:99–112.
2. Cordero RJ, Vij R, Casadevall A. 2017. Microbial melanins for radioprotection and bioremediation. Microb Biotechnol 10:1186–1190.
3. Rajasingham R, Smith RM, Park BJ, Jarvis JN, Govender NP, Chiller TM, Denning DW, Loyse A, Boulware DR. Global burden of disease of HIV-associated cryptococcal meningitis: an updated analysis. Lancet Infect Dis.
4. Eisenman HC, Nosanchuk JD, Webber JBW, Emerson RJ, Camesano TA, Casadevall A. 2005. Microstructure of cell wall-associated melanin in the human pathogenic fungus Cryptococcus neoformans. Biochemistry (Mosc) 44:3683–3693.
5. Nosanchuk JD, Stark RE, Casadevall A. 2015. Fungal Melanin: What do We Know About Structure? Front Microbiol 6.
6. Rosas ÁL, MacGill RS, Nosanchuk JD, Kozel TR, Casadevall A. 2002. Activation of the Alternative Complement Pathway by Fungal Melanins. Clin Diagn Lab Immunol 9:144–148.
7. Wang Y, Aisen P, Casadevall A. 1996. Melanin, melanin "ghosts," and melanin composition in Cryptococcus neoformans. Infect Immun 64:2420–2424.

8. Chatterjee S, Prados-Rosales R, Itin B, Casadevall A, Stark RE. 2015. Solid-state NMR Reveals the Carbon-based Molecular Architecture of Cryptococcus neoformans Fungal Eumelanins in the Cell Wall. J Biol Chem 290:13779–13790.

9. Casadevall A, Nakouzi A, Crippa PR, Eisner M. 2012. Fungal Melanins Differ in Planar Stacking Distances. PLoS ONE 7.

10. Eisenman HC, Frases S, Nicola AM, Rodrigues ML, Casadevall A. 2009. Vesicle-associated melanization in Cryptococcus neoformans. Microbiology 155:3860–3867.

11. Waterman SR, Hacham M, Panepinto J, Hu G, Shin S, Williamson PR. 2007. Cell wall targeting of laccase of Cryptococcus neoformans during infection of mice. Infect Immun 75:714–722.

12. Walker CA, Gómez BL, Mora-Montes HM, Mackenzie KS, Munro CA, Brown AJP, Gow NAR, Kibbler CC, Odds FC. 2010. Melanin externalization in Candida albicans depends on cell wall chitin structures. Eukaryot Cell 9:1329–1342.

13. Walton FJ, Idnurm A, Heitman J. 2005. Novel gene functions required for melanization of the human pathogen Cryptococcus neoformans. Mol Microbiol 57:1381–1396.

14. Idnurm A, Reedy JL, Nussbaum JC, Heitman J. 2004. Cryptococcus neoformans Virulence Gene Discovery through Insertional

Mutagenesis. Eukaryot Cell 3:420–429.

15. Gilbert RG, Hess M, Jenkins AD, Jones RG, Kratochvil P, Stepto RFT. 2009. Dispersity in polymer science (IUPAC recommendations 2009). Pure Appl Chem 81:351–353.

16. Jones RG. 2010. Dispersity in polymer science. Polym Int 59:22–22.

17. Ohki S, Arnold K. 2000. A mechanism for ion-induced lipid vesicle fusion. Colloids Surf B Biointerfaces 18:83–97.

18. Stamatatos L, Leventis R, Zuckermann MJ, Silvius JR. 1988. Interactions of cationic lipid vesicles with negatively charged phospholipid vesicles and biological membranes. Biochemistry (Mosc) 27:3917–3925.

19. Stappers MHT, Clark AE, Aimanianda V, Bidula S, Reid DM, Asamaphan P, Hardison SE, Dambuza IM, Valsecchi I, Kerscher B, Plato A, Wallace CA, Yuecel R, Hebecker B, da Glória Teixeira Sousa M, Cunha C, Liu Y, Feizi T, Brakhage AA, Kwon-Chung KJ, Gow NAR, Zanda M, Piras M, Zanato C, Jaeger M, Netea MG, van de Veerdonk FL, Lacerda JF, Campos A, Carvalho A, Willment JA, Latgé J-P, Brown GD. 2018. Recognition of DHN-melanin by a C-type lectin receptor is required for immunity to *Aspergillus*. Nature 555:382–386.

20. Raposo G, Marks MS. 2007. Melanosomes — dark organelles

enlighten endosomal membrane transport. Nat Rev Mol Cell Biol 8:786–797.

21. Upadhyay S, Xu X, Lowry D, Jackson JC, Roberson RW, Lin X. 2016. Subcellular Compartmentalization and Trafficking of the Biosynthetic Machinery for Fungal Melanin. Cell Rep 14:2511–2518.

22. Franzen AJ, Cunha MML, Miranda K, Hentschel J, Plattner H, da Silva MB, Salgado CG, de Souza W, Rozental S. 2008. Ultrastructural characterization of melanosomes of the human pathogenic fungus Fonsecaea pedrosoi. J Struct Biol 162:75–84.

23. Brown L, Wolf JM, Prados-Rosales R, Casadevall A. 2015. Through the wall: extracellular vesicles in Gram-positive bacteria, mycobacteria and fungi. Nat Rev Microbiol 13:620–630.

24. Gallas JM, Littrell KC, Seifert S, Zajac GW, Thiyagarajan P. 1999. Solution Structure of Copper Ion-Induced Molecular Aggregates of Tyrosine Melanin. Biophys J 77:1135–1142.

25. Eisenman HC, Chow S-K, Tsé KK, McClelland EE, Casadevall A. 2011. The effect of L-DOPA on Cryptococcus neoformans growth and gene expression. Virulence 2:329–336.

26. Seiji M, Fitzpatrick TB. 1961. The Melanosome: A Distinctive Subcellular Particle of Mammalian Melanocytes and the Site of Melanogenesis1. J Invest Dermatol 36:243–252.

27. Barber EJ. 1966. Calculation of density and viscosity of sucrose solutions as a function of concentration and temperature. Natl Cancer Inst Monogr 21:219–239.

28. Schröder M, Schäfer R, Friedl P. 1997. Spectrophotometric determination of iodixanol in subcellular fractions of mammalian cells. Anal Biochem 244:174–176.

29. Kwon-Chung KJ, Polacheck I, Popkin TJ. 1982. Melanin-lacking mutants of Cryptococcus neoformans and their virulence for mice. J Bacteriol 150:1414–1421.

30. Perfect JR. 2000. Cryptococcosis, p. 79–93. *In* Atlas of Infectious Diseases. Current Medicine Group, London.

31. Ellis DH, Pfeiffer TJ. 1990. Natural habitat of Cryptococcus neoformans var. gattii. J Clin Microbiol 28:1642–1644.

32. Emmons CW. 1960. Prevalence of Cryptococcus neoformans in pigeon habitats. Public Health Rep 75:362–364.

33. Neilson JB, Fromtling RA, Bulmer GS. 1977. Cryptococcus neoformans: size range of infectious particles from aerosolized soil. Infect Immun 17:634–638.

34. Powell KE, Dahl BA, Weeks RJ, Tosh FE. 1972. Airborne Cryptococcus neoformans: particles from pigeon excreta compatible with alveolar deposition. J Infect Dis 125:412–415.

35. Maxson ME, Cook E, Casadevall A, Zaragoza O. 2007. The volume and hydration of the Cryptococcus neoformans polysaccharide capsule. Fungal Genet Biol 44:180–186.

36. Cordero RJB, Pontes B, Guimarães AJ, Martinez LR, Rivera J, Fries BC, Nimrichter L, Rodrigues ML, Viana NB, Casadevall A. 2011. Chronological Aging Is Associated with Biophysical and Chemical Changes in the Capsule of Cryptococcus neoformans. Infect Immun 79:4990–5000.

37. Casadevall A, Coelho C, Cordero RJB, Dragotakes Q, Jung E, Vij R, Wear MP. 2018. The Capsule of Cryptococcus neoformans. Virulence 0.

38. Zaragoza O, Rodrigues ML, De Jesus M, Frases S, Dadachova E, Casadevall A. 2009. The capsule of the fungal pathogen Cryptococcus neoformans. Adv Appl Microbiol 68:133–216.

39. Kwon-Chung KJ, Rhodes JC. 1986. Encapsulation and melanin formation as indicators of virulence in Cryptococcus neoformans. Infect Immun 51:218–223.

40. Garcia-Rivera J, Eisenman HC, Nosanchuk JD, Aisen P, Zaragoza O, Moadel T, Dadachova E, Casadevall A. 2005. Comparative analysis of Cryptococcus neoformans acid-resistant particles generated from pigmented cells grown in different laccase substrates. Fungal Genet

Biol 42:989–998.

41. Nosanchuk JD, Rudolph J, Rosas AL, Casadevall A. 1999. Evidence That Cryptococcus neoformans Is Melanized in Pigeon Excreta: Implications for Pathogenesis. Infect Immun 67:5477–5479.

42. Nosanchuk JD, Rosas AL, Lee SC, Casadevall A. 2000. Melanisation of Cryptococcus neoformans in human brain tissue. The Lancet 355:2049–2050.

43. Casadevall A, Rosas AL, Nosanchuk JD. 2000. Melanin and virulence in Cryptococcus neoformans. Curr Opin Microbiol 3:354–358.

44. Frases S, Viana NB, Casadevall A. 2011. Biophysical Methods for the Study of Microbial Surfaces. Front Microbiol 2.

45. Grover WH, Bryan AK, Diez-Silva M, Suresh S, Higgins JM, Manalis SR. 2011. Measuring single-cell density. Proc Natl Acad Sci 108:10992–10996.

46. Biello D, Biello D. 2006. Fact or Fiction?: Archimedes Coined the Term “Eureka!” in the Bath. Sci Am.

47. Kuroki H. 2016. How did Archimedes discover the law of buoyancy by experiment? Front Mech Eng 11:26–32.

48. Baldwin WW, Myer R, Powell N, Anderson E, Koch AL. 1995. Buoyant density ofEscherichia coli is determined solely by the osmolarity of the culture medium. Arch Microbiol 164:155–157.

49. Baldwin WW, Kubitschek HE. 1984. Evidence for osmoregulation of cell growth and buoyant density in Escherichia coli. J Bacteriol 159:393–394.

50. Lowe BA, Miller JD, Neely MN. 2007. Analysis of the Polysaccharide Capsule of the Systemic Pathogen Streptococcus iniae and Its Implications in Virulence. Infect Immun 75:1255–1264.

51. Kubitschek HE. 1987. Buoyant density variation during the cell cycle in microorganisms. Crit Rev Microbiol 14:73–97.

52. Sundqvist G, Figdor D, Hänström L, Sörlin S, Sandström G. 1991. Phagocytosis and virulence of different strains of Porphyromonas gingivalis. Eur J Oral Sci 99:117–129.

53. Sagripanti J-L, Carrera M, Robertson J, Levy A, Inglis TJJ. 2011. Size distribution and buoyant density of Burkholderia pseudomallei. Arch Microbiol 193:69–75.

54. Vijay S, Nair RR, Sharan D, Jakkala K, Mukkayyan N, Swaminath S, Pradhan A, Joshi NV, Ajitkumar P. 2017. Mycobacterial Cultures Contain Cell Size and Density Specific Sub-populations of Cells with Significant Differential Susceptibility to Antibiotics, Oxidative and Nitrite Stress. Front Microbiol 8.

55. Baldwin WW, Kubitschek HE. 1984. Buoyant density variation during the cell cycle of Saccharomyces cerevisiae. J Bacteriol 158:701–704.

56. Allen C, Büttner S, Aragon AD, Thomas JA, Meirelles O, Jaetao JE, Benn D, Ruby SW, Veenhuis M, Madeo F, Werner-Washburne M. 2006. Isolation of quiescent and nonquiescent cells from yeast stationary-phase cultures. J Cell Biol 174:89–100.

57. Kubitschek HE, Baldwin WW, Schroeter SJ, Graetzer R. 1984. Independence of buoyant cell density and growth rate in Escherichia coli. J Bacteriol 158:296–299.

58. Loken MR, Kubitschek HE. 1984. Constancy of cell buoyant density for cultured murine cells. J Cell Physiol 118:22–26.

59. Bryan AK, Goranov A, Amon A, Manalis SR. 2010. Measurement of mass, density, and volume during the cell cycle of yeast. Proc Natl Acad Sci USA 107:999–1004.

60. Kwon-Chung KJ, Bennett JE, Wickes BL, Meyer W, Cuomo CA, Wollenburg KR, Bicanic TA, Castañeda E, Chang YC, Chen J, Cogliati M, Dromer F, Ellis D, Filler SG, Fisher MC, Harrison TS, Holland SM, Kohno S, Kronstad JW, Lazera M, Levitz SM, Lionakis MS, May RC, Ngamskulrongroj P, Pappas PG, Perfect JR, Rickerts V, Sorrell TC, Walsh TJ, Williamson PR, Xu J, Zelazny AM, Casadevall A. 2017. The Case for Adopting the “Species Complex” Nomenclature for the Etiologic Agents of Cryptococcosis. mSphere 2.

61. May RC, Stone NRH, Wiesner DL, Bicanic T, Nielsen K. 2016.

Cryptococcus: from environmental saprophyte to global pathogen. Nat Rev Microbiol 14:106–117.

62. Cogliati M. 2013. Global Molecular Epidemiology of Cryptococcus neoformans and Cryptococcus gattii: An Atlas of the Molecular Types. Scientifica. Research article.

63. O'Meara TR, Alspaugh JA. 2012. The Cryptococcus neoformans Capsule: a Sword and a Shield. Clin Microbiol Rev 25:387–408.

64. Zaragoza O, Casadevall A. 2004. Experimental modulation of capsule size in Cryptococcus neoformans. Biol Proced Online 6:10–15.

65. Frases S, Nimrichter L, Viana NB, Nakouzi A, Casadevall A. 2008. Cryptococcus neoformans Capsular Polysaccharide and Exopolysaccharide Fractions Manifest Physical, Chemical, and Antigenic Differences. Eukaryot Cell 7:319–327.

66. Haynes BC, Skowyra ML, Spencer SJ, Gish SR, Williams M, Held EP, Brent MR, Doering TL. 2011. Toward an Integrated Model of Capsule Regulation in Cryptococcus neoformans. PLOS Pathog 7:e1002411.

67. Zaragoza O, Nielsen K. 2013. Titan cells in Cryptococcus neoformans: cells with a giant impact. Curr Opin Microbiol 16:409–413.

68. McClelland EE, Nicola AM, Prados-Rosales R, Casadevall A. 2010. Ab binding alters gene expression in Cryptococcus neoformans and

directly modulates fungal metabolism. J Clin Invest 120:1355–1361.

69. Cordero RJB, Pontes B, Frases S, Nakouzi AS, Nimrichter L, Rodrigues ML, Viana NB, Casadevall A. 2013. Antibody Binding to Cryptococcus neoformans Impairs Budding by Altering Capsular Mechanical Properties. J Immunol Author Choice 190:317–323.

70. Martinez LR, Moussai D, Casadevall A. 2004. Antibody to Cryptococcus neoformans Glucuronoxylomannan Inhibits the Release of Capsular Antigen. Infect Immun 72:3674–3679.

71. Casadevall A, Cleare W, Feldmesser M, Glatman-Freedman A, Goldman DL, Kozel TR, Lendvai N, Mukherjee J, Pirofski L, Rivera J, Rosas AL, Scharff MD, Valadon P, Westin K, Zhong Z. 1998. Characterization of a Murine Monoclonal Antibody to Cryptococcus neoformans Polysaccharide That Is a Candidate for Human Therapeutic Studies. Antimicrob Agents Chemother 42:1437–1446.

72. Dromer F, Charreire J, Contrepois A, Carbon C, Yeni P. 1987. Protection of mice against experimental cryptococcosis by anti-Cryptococcus neoformans monoclonal antibody. Infect Immun 55:749–752.

73. Casadevall A, Pirofski L. 2004. New Concepts in Antibody-Mediated Immunity. Infect Immun 72:6191–6196.

74. Reynolds CS, Oliver RL, Walsby AE. 1987. Cyanobacterial

dominance: The role of buoyancy regulation in dynamic lake environments. N Z J Mar Freshw Res 21:379–390.

75. Reynolds CS. 2007. Variability in the provision and function of mucilage in phytoplankton: facultative responses to the environment. Hydrobiologia 578:37–45.

76. Bartlett KH, Kidd SE, Kronstad JW. 2008. The emergence of Cryptococcus gattii in British Columbia and the Pacific Northwest. Curr Infect Dis Rep 10:58–65.

77. MacDougall L, Kidd SE, Galanis E, Mak S, Leslie MJ, Cieslak PR, Kronstad JW, Morshed MG, Bartlett KH. 2007. Spread of Cryptococcus gattii in British Columbia, Canada, and Detection in the Pacific Northwest, USA. Emerg Infect Dis 13:42–50.

78. Richardson TL, Jackson GA. 2007. Small Phytoplankton and Carbon Export from the Surface Ocean. Science 315:838–840.

79. Inoue K, Nishimura M, Nayak BB, Kogure K. 2007. Separation of marine bacteria according to buoyant density by use of the density-dependent cell sorting method. Appl Env Microbiol 73:1049–1053.

80. Condie SA, Bormans M. 1997. The Influence of Density Stratification on Particle Settling, Dispersion and Population Growth. J Theor Biol 187:65–75.

81. Kidd SE, Bach PJ, Hingston AO, Mak S, Chow Y, MacDougall L,

Kronstad JW, Bartlett KH. 2007. Cryptococcus gattii Dispersal Mechanisms, British Columbia, Canada. Emerg Infect Dis 13:51–57.

82. Kidd SE, Chow Y, Mak S, Bach PJ, Chen H, Hingston AO, Kronstad JW, Bartlett KH. 2007. Characterization of Environmental Sources of the Human and Animal Pathogen Cryptococcus gattii in British Columbia, Canada, and the Pacific Northwest of the United States. Appl Environ Microbiol 73:1433–1443.

83. Rivera J, Feldmesser M, Cammer M, Casadevall A. 1998. Organ-Dependent Variation of Capsule Thickness in Cryptococcus neoformans during Experimental Murine Infection. Infect Immun 66:5027–5030.

84. Noverr MC, Williamson PR, Fajardo RS, Huffnagle GB. 2004. CNLAC1 Is Required for Extrapulmonary Dissemination of Cryptococcus neoformans but Not Pulmonary Persistence. Infect Immun 72:1693–1699.

85. MacGill TC, MacGill RS, Casadevall A, Kozel TR. 2000. Biological Correlates of Capsular (Quellung) Reactions of Cryptococcus neoformans. J Immunol 164:4835–4842.

86. Nimrichter L, Frases S, Cinelli LP, Viana NB, Nakouzi A, Travassos LR, Casadevall A, Rodrigues ML. 2007. Self-Aggregation of Cryptococcus neoformans Capsular Glucuronoxylomannan Is

Dependent on Divalent Cations. Eukaryot Cell 6:1400–1410.

87. Roe CC, Bowers J, Oltean H, DeBess E, Dufresne PJ, McBurney S, Overy DP, Wanke B, Lysen C, Chiller T, Meyer W, Thompson GR, Lockhart SR, Hepp CM, Engelthaler DM. 2018. Dating the Cryptococcus gattii Dispersal to the North American Pacific Northwest. mSphere 3.

88. Pertoft H, Rubin K, Kjellén L, Laurent TC, Klingeborn B. 1977. The viability of cells grown or centrifuged in a new density gradient medium, Percoll(TM). Exp Cell Res 110:449–457.

89. Pertoft H. 2000. Fractionation of cells and subcellular particles with Percoll. J Biochem Biophys Methods 44:1–30.

90. Dragotakes Q, Casadevall A. 2018. Automated Measurement of Cryptococcal Species Polysaccharide Capsule and Cell Body. J Vis Exp JoVE.

91. Bryan AK, Hecht VC, Shen W, Payer K, Grover WH, Manalis SR. 2014. Measuring single cell mass, volume, and density with dual suspended microchannel resonators. Lab Chip 14:569–576.

92. SZATANEK R, BARAN J, SIEDLAR M, BAJ-KRZYWORZEKA M. 2015. Isolation of extracellular vesicles: Determining the correct approach (Review). Int J Mol Med 36:11–17.

93. R. Watt AA, P. Bothma J, Meredith P. 2009. The supramolecular

structure of melanin. Soft Matter 5:3754–3760.

94. d'Ischia M, Wakamatsu K, Napolitano A, Briganti S, Garcia-Borron J-C, Kovacs D, Meredith P, Pezzella A, Picardo M, Sarna T, Simon JD, Ito S. 2013. Melanins and melanogenesis: methods, standards, protocols. Pigment Cell Melanoma Res 26:616–633.

95. Rosas ÁL, Nosanchuk JD, Casadevall A. 2001. Passive Immunization with Melanin-Binding Monoclonal Antibodies Prolongs Survival of Mice with Lethal Cryptococcus neoformans Infection. Infect Immun 69:3410–3412.

96. Schweitzer AD, Revskaya E, Chu P, Pazo V, Friedman M, Nosanchuk JD, Cahill S, Frases S, Casadevall A, Dadachova E. 2010. Melanin-Covered Nanoparticles for Protection of Bone Marrow During Radiation Therapy of Cancer. Int J Radiat Oncol 78:1494–1502.

97. Yan J, Ji Y, Zhang P, Lu X, Fan Q, Pan D, Yang R, Xu Y, Wang L, Zhang L, Yang M. 2016. Melanin nanoparticles as an endogenous agent for efficient iron overload therapy. J Mater Chem B 4:7233–7240.

RAGHAV VIJ

500 West University Parkway, Apt 12 L, Baltimore, MD, 21210

Phone: +1 443-500 (9960) • E-Mail: rvij3@jhmi.edu

EDUCATION

- Sc.M., Molecular Microbiology and Immunology (MMI) 2016-18, Johns Hopkins Bloomberg School of Public Health, Johns Hopkins University CGPA 3.68/4 as of Term 2 (2nd year), 2017.
- B. Tech, Biotechnology 2011-15, Amity Institute of Biotechnology (AIB), Amity University CGPA 6.73/10 (WES, 3.22/4)

PROJECTS UNDERTAKEN

- Sc.M. Thesis, Dr. Arturo Casadevall Lab, Molecular Microbiology and Immunology, 2016-2018 (November 2016-March 2018). Isolating and characterizing the unit of fungal melanin in *Cryptococcus neoformans*. The effect of cell wall associated virulence factors on the buoyant cell density of *C. neoformans*
- National Network for Mathematical & Computational Biology (NNMCB), Birla Institute of Technology, (8 weeks) July 2015, Dr. Ashoke Sharon Lab. Molecular docking & dynamics simulation to understand molecular basis of possible calsequestrin modulator.
- Amity Institute of Environmental Toxicology Safety Management, Dr. Tanu Jindal Lab, Final B. Tech Dissertation (12 weeks). February 2015. Evaluation of insecticidal activity of methanol extract of *Calotropis procera* against *Callosobruchus maculatus*.
- AIB Summer Project (8 weeks) May 2014. Dr. V. R. Pooja, Efficacy of plant extracts on *C. neoformans* with special emphasis on melanin synthesis.
- School of Health Sciences, Dr. Anita Kar lab, Pune University, Pune - Summer Project (6 weeks) May 2013. Epidemiological and genetic study on Beta-thalassemia.

ADDITIONAL EXPERIENCE

- Seminar talk on "*C. neoformans* polysaccharide capsule and melanin: two major virulence factors" at NIST (National Institute of Standards and Technology), Center for Neutron Research.
- Participation in poster presentation on "Molecular dynamic simulation to study the conformational changes in the ATP lid of Hsp90" at "Recent trends in Affordable and Sustainable Drug Discovery and Development", (2016) an international conference by Indian Society of Chemists and Biologists.
- Graduate Aptitude Test in Engineering (GATE) 2015, Biotechnology qualified and rank holder.

- Participation in International Symposium on 'Accelerating Biology 2013: The Next Wave' Centre for Development of Advanced Computing (C-DAC).
- Participation in poster presentation on "Antimicrobial potential and phytochemical analysis of *Viola odarata* leaves" at "Use of Animals and Alternatives on Biomedical Research with Special reference to Drug Discovery and Drug Development", (2013) a national conference under the aegis of Committee of Control and Supervision of Experiments on Animals (CPSCEA).
- Volunteered for research under Dr. Praveen Dahiya, faculty at Amity University on the anti-microbial properties of plant *Viola odarota*, (2013).

PUBLICATION

- Cordero, R. J., **Vij, R.**, & Casadevall, A. (2017). Microbial melanins for radioprotection and bioremediation. *Microbial Biotechnology*, 10(5), 1186-1190.
- Coelho, C., Brown, L., **Vij, R.**, Maryam, M., Burnet, M. C., Kyle, J. E., Heyman, H. M., Ramirez J., Rosales, R.P., Lauvau, G., Nakayasu, E.S., Brady, N.R., Brady, A., Coppens, I. and Casadevall, A. (2017). Listeria monocytogenes virulence factors are secreted in biologically active Extracellular Vesicles. *bioRxiv*, 210906. In submission to JBC.
- Casadevall, A., Coelho, C., Cordero, R. J., Dragotakes, Q., Jung, E., **Vij, R.,** & Wear, M. P. (2018). The Capsule of Cryptococcus neoformans. *Virulence*, (just-accepted), 00-00.
- Under review (*mSphere*): **Vij, R.**, Cordero, R. J., Casadevall, A. Eureka! The Buoyant cell density of Cryptococcus neoformans is affected by growth conditions, capsule size and antibody binding.
- In preparation: Vij, R., Camacho, E., Cordero, R.J., Casadevall, A. Isolation and characterization of fungal unit of melanin from *C. neoformans*.

SKILLS

Computational skills include: C, C++, SQL, MS Office, STATA, Prism

EXTRACURRICULAR ACTIVITIES

- Deputy Secretary to International Press at Amity International Model United Nations 2015.
- President (2014-15) and Scriptwriter at "English Dramatics Society of AIB: TheaTORS". Participated as an actor for the society in college festivals, as well as a sound technician, stage manager and director, and won several prizes with the team.
- Head Co-coordinator AIB Literary Club (2014-15) - Participation at college festivals IIT Delhi Literati (2011, 2013).
- Trained in Indian classical music (tabla and vocals). Appeared for Gandharva Mahavidyalaya examinations for vocals (2 exams) and tabla (3 exams).